The Prevalence of Killer Yeasts in the Gardens of Fungus-Growing Ants and the Discovery of a Novel Killer Toxin named Ksino.

Rodolfo Bizarria Jr.[a,b], Jack W. Creagh[a], Renato A. Corrêa dos Santos[c], Lily LGivens, Sarah A. Coss[a], Tanner J. Badigian[a], Adrian V. Chavez[a], Rim T. Tekle[a], Noah Fredstrom[d], F. Marty Ytreberg[e.f], Maitreya J. Dunham[d], Andre Rodrigues[b]*, Paul A. Rowley[a,f]*

[a]Department of Biological Sciences, University of Idaho, Moscow, Idaho, USA.

[b]Department of General and Applied Biology, São Paulo State University (UNESP), Institute of Biosciences, Rio Claro, São Paulo, Brazil.

[c]Laboratory of Computational, Evolutionary, and Systems Biology, Center for Nuclear Energy in Agriculture, University of São Paulo (USP), Piracicaba, São Paulo, Brazil

[d]Department of Genome Sciences, University of Washington, Seattle, WA 98195, USA.

[e]Department of Physics, University of Idaho, Moscow, ID, 83844, USA.

[f]Institute for Modeling Collaboration and Innovation, University of Idaho, Moscow, ID, 83844, USA.

*Corresponding authors

Abstract

Killer toxins are proteinaceous antifungal molecules produced by yeasts, with activity against a wide range of human and plant pathogenic fungi. Fungus gardens of attine ants in Brazil were surveyed to determine the presence of killer toxin-producing yeasts and to define their antifungal activities and ecological importance. Our results indicate that 10 out of 59 yeasts species isolated from fungal gardens are killer yeasts. Killer yeasts were less likely to inhibit the growth of yeasts isolated from the same environment but more effective at inhibiting yeast isolated from other environments, supporting a role for killer yeasts in shaping community composition. All killer yeasts harbored genome-encoded killer toxins lacked cytoplasmic

toxin-encoding elements (i.e., double-stranded RNA satellites and linear double-stranded DNAs). Of all the killer yeasts associated with attine ants, *Candida sinolaborantium* (strain LESF 1467) showed a broad spectrum of antifungal activities against 39 out of 69 57% of yeast strains tested for toxin susceptibility. The complete genome sequence of *C. sinolaborantium* LESF 1467 identified a new killer toxin, Ksino, with similarities in primary sequence and tertiary structure to the *Saccharomyces cerevisiae* killer toxin named Klus. Surveys of publicly available genome databases identified homologs of Ksino in the genomes of yeast strains of *Saccharomycetes* and *Pichiomycetes*, as well as other species of Ascomycota and Basidiomycota filamentous fungi. This demonstrates that killer yeasts can be widespread in attine ant fungus gardens, possibly influencing fungal community composition and the importance of these complex microbial communities for discovering novel antifungal molecules.

Keywords: Killer yeasts, Killer toxins, Antifungals, Budding yeast, Fungus-growing ants

Importance

Attine ants perform essential ecosystem services through the harvesting of substrates for fungiculture. The cultured fungi are a food source for attine ants. Characterizing antifungal toxin-producing yeasts (killer yeasts) is vital to understanding how they might protect gardens from invasion by unwanted fungal species. This study describes a new toxin named Ksino from the yeast *Candida sinolaborantium*, a member of a new group of toxins found across many different species of fungi. This work supports the role of killer yeasts in the ecology of fungicultures and competition between fungi. The observed high prevalence of killer yeasts in fungal gardens also enables the discovery of novel antifungal molecules with the potential to be applied against disease-causing fungi.

1. Introduction

Killer yeasts were first described in *Saccharomyces cerevisiae* in the 1960s (Makower and Bevan, 1963; Woods and Bevan, 1968), after which many strains and species of yeasts and yeast-like fungi were also observed to secrete antifungal killer toxins (Woods and Bevan, 1968;

Golubev et al., 2002; Pfeiffer et al., 2004; Koltin and Day, 1976; Castillo and Cifuentes, 1994). Killer toxins can have a range of antifungal activities ranging from narrow to broad specificities, affecting cells from close or distantly related fungal species (Boynton, 2019; Golubev, 1998; Golubev, 2006). The prevalence of killer yeasts strains in natural environments is reported between 5% to 33% for positive killer phenotypes (Philliskirk and Young, 1975; Stumm et al., 1977; Starmer et al., 1987; Abranches et al. 1997, Abranches et al. 1998; Trindade et al. 2002; Pieczynska et al., 2013; Wojcik and Kordowska-Wiater, 2015) but can also be as high as 59% in yeast associated with wine production (Hidalgo and Flores, 1994). Killer toxins are known to be active against human and plant pathogenic yeasts (Middelbeek et al. 1980; Hodgson et al. 1995; Buzzini et al., 2001; Giovati et al., 2018) and can control spoilage organisms that are important for agriculture and food industry (Walker et al., 1995; Chessa et al., 2017). The rise in acquired drug resistance and the emergence of drug-resistant fungal pathogens justifies the search for novel antifungal killer toxins from diverse natural environments, including insect-associated fungal communities.

Killer yeast communities have been previously reported in fungus-growing ant colonies (Hymenoptera: tribe Attini: subtribe Attina, hereafter called ‘attine ants’). Attine ants established a long-term obligate mutualism with basidiomycete fungi in the *Agaricaceae* and *Pterulaceae* families, using them as the primary source of food for their colonies (Branstetter et al., 2017; Nygaard et al., 2016; Schultz and Brady, 2008, Möller, 1893; Weber, 1972). According to their cultivars and foraging substrates, each species approaches fungiculture differently, and these interactions are considered a model for studying the evolution of mutualisms (Schultz and Brady, 2008, Schultz et al., 2015). Moreover, attine ants are key ecological agents in the Neotropics as dominant herbivores, promoting nutrient cycling, soil fertility, and seed dispersal (Corrêa et al., 2010; Meyer et al., 2011, Farji-brener and Werenkraut, 2015; Sternberg et al., 2007; Leal and Oliveira, 1998). The foraging behavior of attine ants also contributes to the presence of a large and complex community of environmental yeasts in fungus gardens (Craven et al. 1970; Fisher et al., 1996; Pagnocca et al., 2008; Arcuri et al., 2014; Bizarria Jr. et al., 2022). Fungus gardens are likely an important source of new killer toxins due to the high concentration of simple sugars (Silva et al., 2003, Silva et al., 2006), a large density of yeasts and filamentous fungi (Fisher et al., 1996; Craven et al., 1970; Pagnocca et al., 1996; Rodrigues et al., 2008; Bizarria Jr. et al., 2022), and the hypothesized role on garden "immunity" by yeasts (Rodrigues et al. 2009) – all key elements for species competition (Boynton, 2019). Killer yeasts are primarily associated with the basidiomycete

91 fungus farmed by attine ants, the bodies of ants, and the leaves foraged by the ants (Carreiro et
92 al. 2002; Robledo-Leal et al. 2016; Bizarria Jr. et. al. 2023). In prior studies, killer positive
93 phenotypes have been identified in 5% to 11% of the interactions between yeasts derived from
94 attine ant fungus gardens (Carreiro et al. 2002; Bizarria Jr. et. al. 2023).

95 Killer toxins can modify the community composition of yeasts as an outcome of
96 competition or cooperation between killer yeasts, killer toxin-susceptible yeasts, and killer
97 toxin-resistant yeasts that are determined by spatial distribution, pH, and ploidy (Károlyi et al.,
98 2005; McBride et al. 2008; Wloch-Salamon et al. 2008). Killer toxin production also plays a
99 potential role in yeast dispersal, resource consumption among species, and invade or prevent
100 invasions from competitors (Boynton, 2019; Buser et al., 2021; Pintar and Starmer, 2003;
101 Ganter and Starmer, 1992; Travers-Cook et al., 2023). The coexistence of the different
102 phenotypes is known to be affected by environmental parameters, including nutrient
103 availability (Pintar and Starmer, 2003; Wloch-Salamon et al. 2008), cell density (Greig and
104 Travisano 2008; Vadasz et al. 2003), pH, and temperature (Bussey et al. 1988; McBride et al.
105 2008; Magliani et al. 1997), which can reflect the production and distribution of killer toxins
106 in spatially structured environments (Boynton, 2019; Giometto et al. 2021; Kerr et al. 2002;
107 Libberton et al. 2015; Wloch-Salamon et al. 2008). On the other hand, killer toxins are often
108 reported to play a role in interference competition in environments that enforce the interaction
109 between toxin-producing and neighboring susceptible cells (such as well-mixed habitats like
110 laboratory co-cultures and wine fermentation, changing the community structure and function,
111 as an outcome of competition or cooperation between killer yeasts, killer toxin-susceptible
112 yeasts, and killer toxin-resistant yeasts (Bussey et al., 1988; Hidalgo and Flores, 1994;
113 Pieczynska et al., 2016; Boynton, 2019).

114 Killer toxins are encoded by different genetic elements, including chromosomal genes,
115 extrachromosomal elements (such as non-autonomous double-stranded RNA (dsRNA)
116 satellites that are maintained by mycoviruses), and autonomous linear double-stranded DNAs
117 (dsDNA) (Bevan et al., 1973; Somers and Bevan, 1969; Magliani et al., 1997; Rowley, 2017).
118 DsRNA satellites have been previously found to be associated with *Hanseniaspora uvarum*,
119 *Pichia kluyveri*, *Saccharomyces* spp., *Torulaspora delbrueckii*, and *Zygosaccharomyces bailii*
120 (Ivannikova et al 2006, Ivannikova et al 2007; Naumov et al., 2009; Schmitt and Neuhausen,
121 1994; Ramírez et al., 2015; Rodríguez-Cousiño et al., 2017; Zorg et al., 1988), while dsDNA
122 plasmids have been identified in the genera *Babjevia, Debaryomyces*, *Kluyveromyces*,

123 *Millerozyma*, and *Pichia* (Klassen and Meinhardt 2007; Schaffrath et al. 2018; Klassen et al.
124 2017). The association of the killer phenotype with the presence of dsRNA satellites has been
125 most thoroughly studied in *S. cerevisiae* (Crabtree et al., 2023; Vijayraghaven et al., 2023). For
126 example, in a survey of 1,270 *S. cerevisiae* isolates, the frequency of killer yeasts was 50%,
127 and 60% of these killer yeasts had dsRNA satellites (Crabtree et al., 2023). Killer toxin
128 production by the remaining 40% of killer yeasts was closely correlated with the chromosomal
129 killer toxin gene *KHS1*. Considering the many killer yeasts described, only a few studies have
130 defined chromosomal genes that encode the toxins responsible for the observed antifungal
131 effects. Chromosomally encoded killer toxins and their homologs, including K1-like (KKT
132 killer toxins), KHR, KHS, SMKT, KP4-like, PMKT, and other *Pichia* toxins, have been
133 described in many different species of fungi (Goto et al., 1990; Goto et al., 1991; Suzuki and
134 Nikkuni, 1994; Belda et al., 2017, Fredericks et al. 2021, Brown 2011, Lu and Faris 2019).
135 Despite the prevalence of genomic-encoded toxins, some dsRNA satellite-encoded toxins were
136 observed to have genomic homologs in different Saccharomycotina lineages (Frank and Wolfe,
137 2009; Fredericks et al., 2021). However, the frequency of killer yeasts and the prevalence of
138 dsRNA satellites and dsDNA extrachromosomal elements in different lineages of
139 Saccharomycotina and yeast-like fungi is still understudied.

140 In this study, we explore the nature and prevalence of the killer phenotype in different
141 Saccharomycotina lineages associated with attine ant fungus gardens, which are habitats that
142 are rich in yeasts, shedding light on their putative ecological role in this environment (Bizarria
143 Jr. et al. 2023). It was revealed that fungus gardens harbor diverse killer yeasts with narrow
144 and broad antifungal activities. Unlike the well-studied killer yeasts of the *Pichia* and the
145 *Saccharomyces* genera, attine ant-associated killer yeasts were devoid of cytoplasmic toxin-
146 encoding elements such as linear dsDNA plasmids and dsRNA satellites (Magliani et al., 1997;
147 Marquina et al., 2002). Therefore, to identify the gene(s) responsible for killer toxin production,
148 a genome mining approach was used by determining the whole genome sequence of the killer
149 yeast *Candida sinolaborantium* that displayed a broad spectrum of antifungal activities against
150 many species of yeasts, including human pathogens. This approach identified a new killer toxin
151 named Ksino. This novel killer toxin has homologs in both yeasts and filamentous fungi and
152 shares a similar antifungal activity and predicted structure to an *S. cerevisiae* killer toxin named
153 Klus. Collectively, it was found that fungus gardens of attine ants can be used to explore the
154 ecological role of killer yeasts and discover new killer toxins for possible future application as
155 natural antifungals.

2. Results

Fungus gardens of attine ants harbor killer yeasts. To assess the diversity of yeasts associated with fungus-growing ants and their potential for antifungal toxin production, fungus gardens of four ant fungiculture systems were surveyed from 28 nests from four cities in Brazil (Fig. 1A; Table S1). The ant species included the leaf-cutting ant *Acromyrmex coronatus*, the non-leaf-cutting ant *Mycetomoellerius tucumanus*, and the lower attines *Mycetophylax* aff. *auritus* and *Mycocepurus goeldii* that cultivate Agaricaceae fungi, and *Apterostigma goniodes* that cultivates Pterulaceae fungi (Fig. 1B). Ants were selected to broadly represent different fungiculture systems, foraging and preparation behaviors, and the yeast microbiota associated with fungus gardens. Yeasts were isolated from fungus gardens by culturing on synthetic growth media. Microsatellite amplification, sequencing of the D1/D2 domain of the large subunit ribosomal RNA gene, and phylogenetic reconstruction were used for taxonomy. The 180 isolated yeast strains comprised 59 species belonging to eight families and six orders from the Saccharomycotina subphylum previously characterized in a large study of yeasts and yeast-like fungi associated with fungus gardens of attine ants (Fig. 1C; Table S1) (Bizarria Jr. et al., 2023). Of the yeasts isolated, 91 were associated with *Acromyrmex coronatus*, 13 with *Mycetomoellerius tucumanus*, 42 with *Mycetophylax* aff. *auritus*, 25 with *Mycocepurus goeldii*, and nine with *Apterostigma goniodes* (Table S1) (Bizarria Jr. et al., 2023).

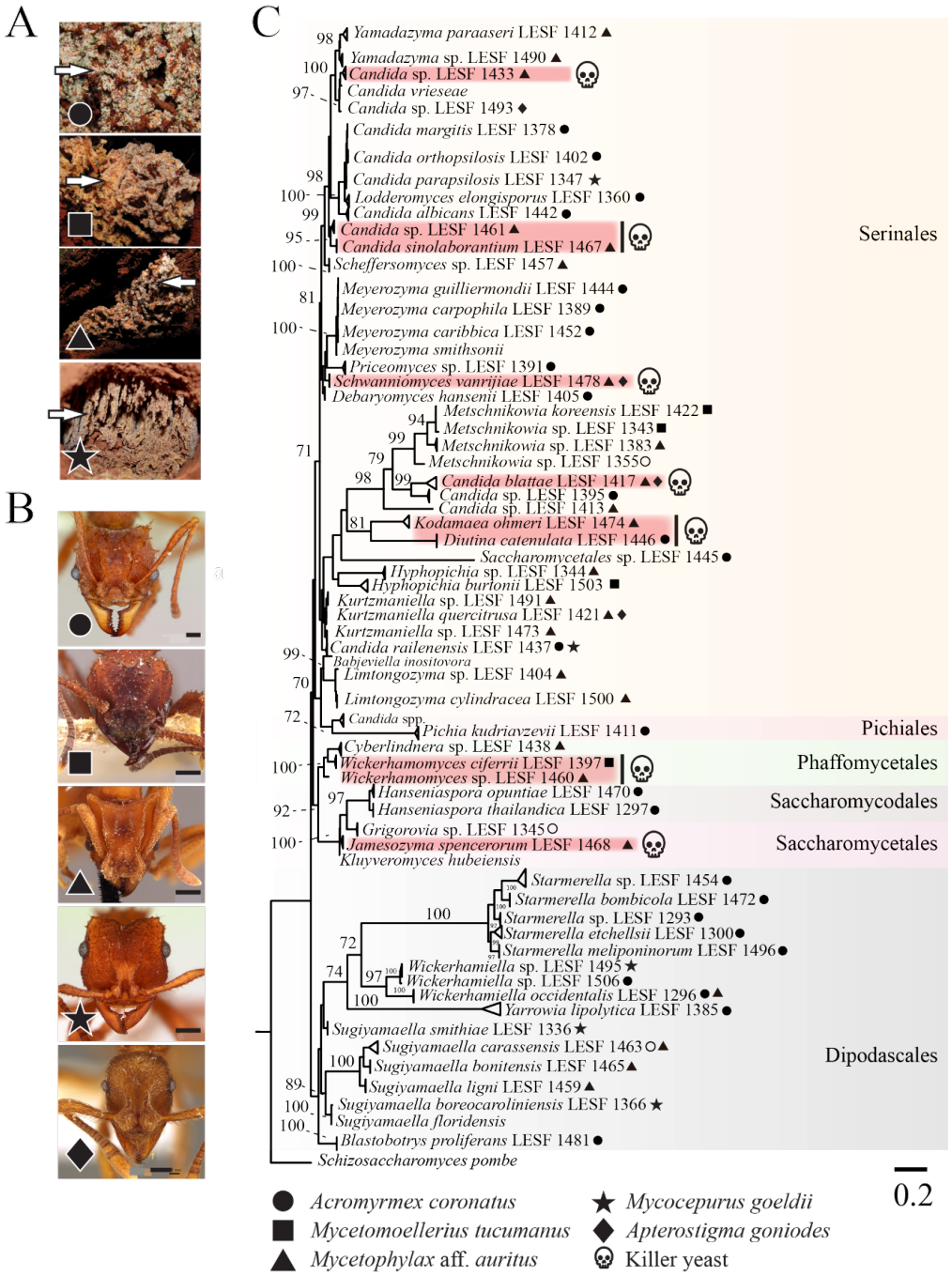

FIG 1. Fungus gardens of different attine ants harbor different killer yeasts. **A.** Images of fungus gardens of different ant species from which yeasts were isolated (arrowheads). The gardens of the leaf-cutting ant *Acromyrmex coronatus* (circle), the non-leaf-cutting ant *Mycetomoellerius tucumanus* (square), the lower attines *Mycetophylax* aff. *auritus* (triangle), and *Mycocepurus goeldii* (star). The fungus garden of *Apterostigma goniodes* is not represented. **B.** Representative images of attine ant species: *Acromyrmex coronatus* (CASENT0173791, April Nobile) (circle); *Mycetomoellerius tucumanus* (CASENT0909391, Will Ericson) (square); *Mycetophylax auritus* (CASENT0901666, Ryan Perry) (triangle), *Mycocepurus goeldii* (CASENT0173988, April Nobile) (star), and *Apterostigma goniodes* (CASENT0922040, Michele Esposito (diamond). The scale bar on all images represents 0.2 mm. Photos of ants were downloaded from "www.antweb.org." **C**. Phylogenetic relationship of yeasts isolated from fungal gardens as inferred by maximum likelihood and the rRNA gene. Symbols in tree leaves indicate the isolation source of yeasts, as depicted in panels A and B. Red shading and skulls denote the species confirmed as killer yeasts. The phylogenetic clades were highlighted by order following the updated classification

194 for the Saccharomycotina proposed by Groenewald et al., (2023) and www.mycobank.org. *Schizosaccharomyces*
195 *pombe* was positioned as an outgroup. The number on the branches are ultrafast bootstrap values (values higher
196 than 70 are shown), and the scale bar denotes the number of nucleotide substitutions per site.

197

198 From the 59 yeast species identified that were associated with attine ant gardens, ten
199 species had isolates that were able to produce killer toxins (10 out of 59; 17% of killer yeasts)
200 (Fig. 1C). Killer toxin production was scored by the absence of growth around a killer yeast or
201 the staining of the lawn yeast with the redox indicator methylene blue (as an indicator of cell
202 death) at pH 4.6. This pH was used as many previously described killer toxins are active in
203 these conditions and it is close to the pH observed in fungus gardens where these yeasts were
204 isolated (pH 5.1-5.4). The identified killer yeasts were effective at inhibiting strains that were
205 either previously determined to be susceptible to killer toxins (Fredericks et al., 2021), human
206 pathogenic yeasts, or yeasts randomly selected from fungus gardens and other sources (Fig. 2A
207 and S1; File S1). From the attine ant gardens, *Candida blattae*, *Candida sinolaborantium*,
208 *Candida* sp. (closest to *Candida temnochilae*), *Candida* sp. (closest to *Candida*
209 *membranifaciens*), *Diutina catenulata*, *Jamesozyma spencerorum*, *Kodamaea ohmeri*,
210 *Schwanniomyces vanrijiae*, *Wickerhamomyces ciferrii*, and *Wickerhamomyces* sp. (closest to
211 *Wickerhamomyces rabaulensis*) were identified as killer yeasts. These yeasts had unique
212 antifungal activities when compared to other previously identified *Saccharomyces* killer toxins
213 (K1, K1L, K2, K21, K28, K45, K62, K74, and Klus), as has been observed in a previous screen
214 for killer yeasts of *S. cerevisiae* (Crabtree et al., 2023). Killer yeasts were only absent from the
215 fungus gardens of *M. goeldii*, but were recovered from the fungus gardens of *Acromyrmex*
216 *coronatus* (7% killer yeasts, 6 out of 91 isolates), *Mycetomoellerius tucumanus* (46%, 6 out of
217 13), *Mycetophylax* aff. *auritus* (43%, 18 out of 42), and *Apterostigma goniodes* (22%, 2 out of
218 9) (Fig. 2B). Thirty-two out of 180 (18%) yeasts from attine ants were also capable of inhibiting
219 the growth of susceptible yeasts, including human pathogenic yeasts such as *Candida albicans*,
220 *Candida glabrata*, and *Candida auris* (Fig. S1). The attine ant-associated killer yeasts *J.*
221 *spencerorum* LESF 1468 and *S. vanrijiae* LESF 1521 could only inhibit the growth of
222 pathogenic yeasts (Fig. S1, File S1). Many killer yeasts from the same species had similar
223 antifungal activities as demonstrated by their phenotypic clustering (see *Candida* sp. closest to
224 *C. temnochilae*, *C. blattae*, *D. catenulata*, *S. vanrijiae*, *Wickerhamomyces* sp. closest to *W.*
225 *rabaulensis*, and *W. ciferrii*) (Fig. 2A). Specifically, *Candida blattae* killer yeasts had similar
226 antifungal activities even when isolated from the fungicultures of different ant species
227 (compare *Candida blattae* isolates from *Mycetophylax* aff. *auritus* and *Apterostigma goniodes*)

228 (Fig. 2A). However, there were isolates of *S. vanrijiae* killer yeasts from the fungiculture of
229 *Mycetophylax* aff. *auritus* with strikingly different spectra of antifungal activities, which
230 suggests that isolates of the same species were not always clonal. *Candida sinolaborantium*
231 (strain LESF 1467) had the broadest range of antifungal activity, inhibiting 57% of all 69 lawn
232 strains tested (Fig. 2A and S1, File S1). Comparing interactions between ant-associated killer
233 yeasts and susceptible lawn strains from fungus gardens and other environmental sources found
234 that growth inhibition was more prevalent for yeasts from different sources (Chi-squared test,
235 p-value < 0.01) (Fig. 2C; Table S2). Specifically, only 1% (6 of 647) of interactions between
236 ant-associated yeasts from the same type of fungiculture resulted in growth inhibition. In
237 contrast, 4% (301 of 8,353) of interactions between ant-associated killer yeasts and yeasts from
238 fungus gardens and other environmental sources isolation sources resulted in growth inhibition.
239
240 The ability to produce killer toxins is often associated with the presence of linear
241 dsDNA plasmids or mycovirus-associated dsRNA satellites. We assayed all attine ant-
242 associated killer yeasts for the presence of these genetic elements using solvent extraction of
243 nucleic acids, cellulose chromatography, and gel electrophoresis (Crabtree et al., 2019). In
244 particular, the use of cellulose chromatography selectively enriches dsRNAs derived from
245 mycoviruses and satellites, reducing the false negative rate compared to solvent extraction
246 alone and without the bias of reverse-transcriptase PCR (Crabtree et al., 2023). However, we
247 did not find that any of the isolated attine ant-associated strains possess dsRNAs (i.e., viruses
248 and satellites) or dsDNA cytoplasmic elements (i.e., plasmids). Double-stranded RNA viruses
249 have been found in many different species of yeasts without satellite dsRNAs (Crucitti et al.,
250 2021; Lee et al., 2022; Taylor et al., 2013); thus we broadened the survey to include all attine-
251 associated yeasts but again did not identify any dsRNA viruses. This suggested that the killer
252 toxins associated with yeasts from fungus gardens are genome-encoded and that dsRNA
253 viruses, dsRNA satellites, and DNA plasmids were not observed in yeasts associated with attine
254 ant species in the geographical area sampled.
255

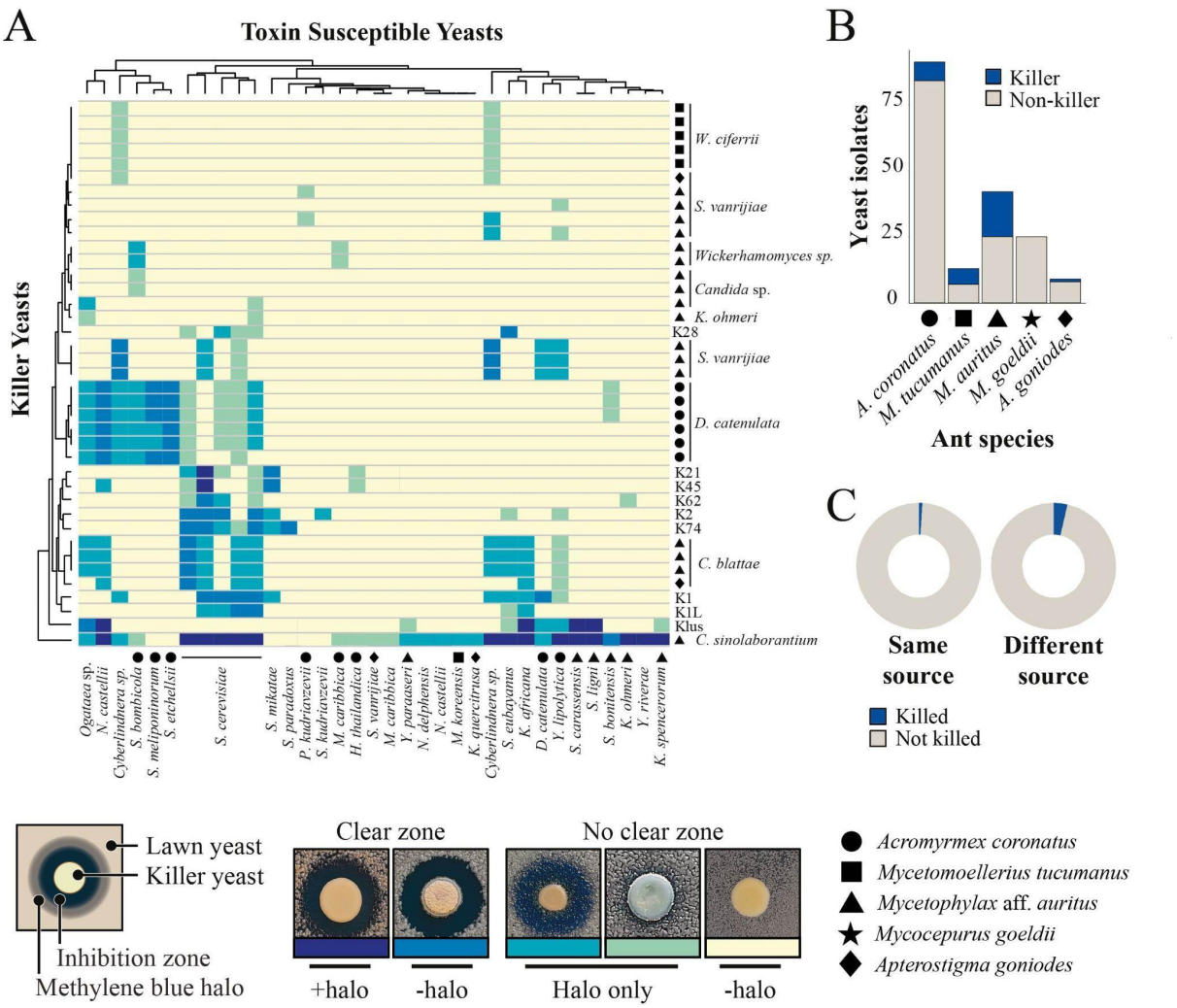

FIG 2. Killer yeasts from fungus gardens have unique spectra of antifungal activity. A. Heatmap with the interactions between canonical *Saccharomyces* killer yeasts (K1, K1L, K2, Klus, K21, K28, K45, K62, K74), killer yeasts associated with ants, and killer toxin susceptible strains. Origins of the ant-associated killer yeasts; *Acromyrmex coronatus* (circle); *Mycetomoellerius tucumanus* (square); *Mycetophylax* aff. *auritus* (triangle), *Apterostigma goniodes* (diamond). Killer toxin activity was qualitatively assessed based on the presence and size of growth inhibition zones and/or methylene blue staining around killer yeasts (representative images of these phenotypes are shown). Darker colors on the heatmap represent a more prominent killer phenotype, with yellow indicating no observable killer phenotype. Clusters on the dendrograms connecting individual killers or susceptible yeasts indicate similar susceptibilities to killer toxins or antifungal activities. **B.** Number of killer yeasts and non-killers associated with the different attine ant fungicultures. **C**. Number of killer toxin-positive and negative interactions between yeast from attine ant environment and susceptible strains (Table S1.), growth inhibition by killer yeasts is different among the same or different fungicultures and locations.

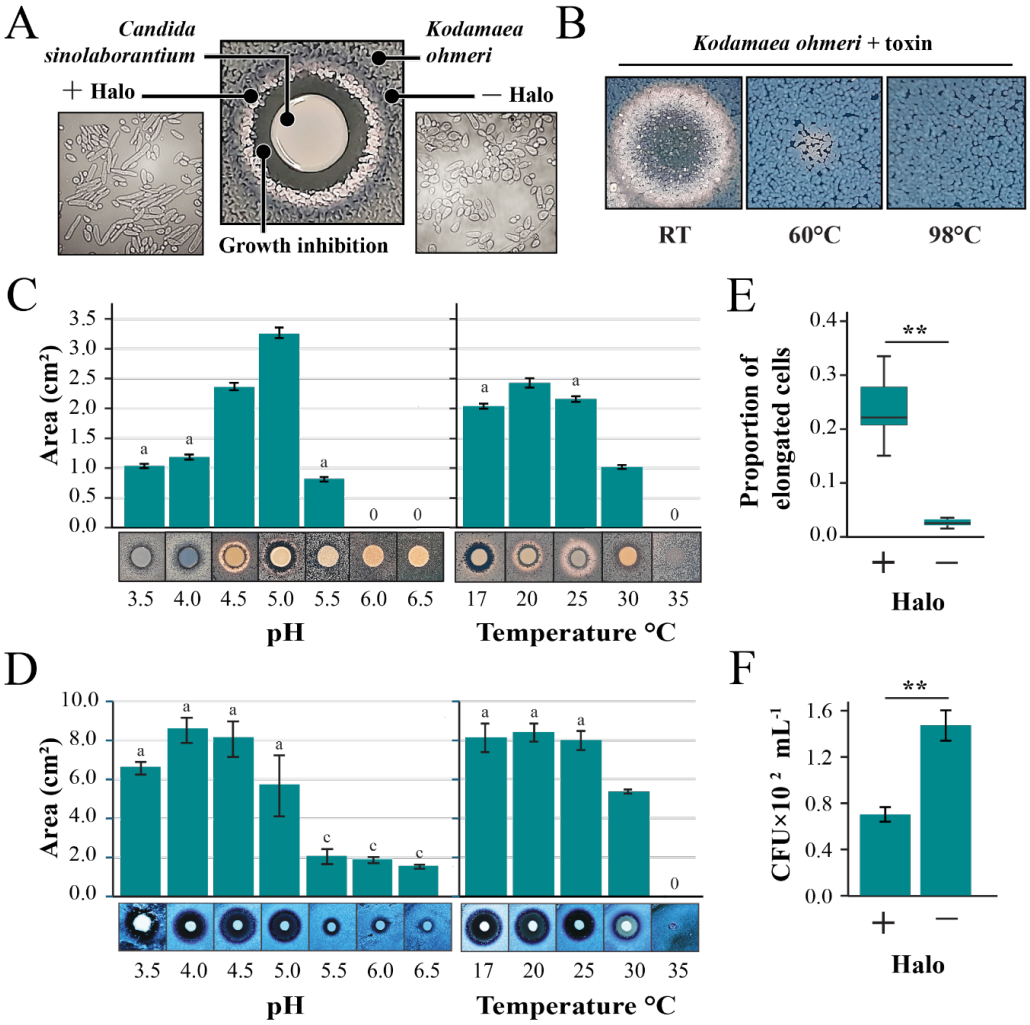

FIG 3. The antifungal activities of *Candida sinolaborantium*. A. Growth phenotypes associated with the co-culture of the killer yeast *C. sinolaborantium* with *K. ohmeri* at room temperature (RT) and pH 4.6. Cell morphology of *K. ohmeri* inside (+Halo) and outside (-Halo) the white halo around *C. sinolaborantium* was evaluated by microscopy. **B**. The antifungal activity of protein precipitates derived from the spent growth medium of *C. sinolaborantium* and the heat stability of these activities at 60ºC and 98ºC. Killer yeast activity of *C. sinolaborantium* under different pH and temperature conditions against **C.** *K. ohmeri* and *C. castelli*. For all pH and temperature data, the means were significantly heterogeneous (one-way anova, P<0.01). Means with the same letter are not significantly different from each other (Tukey–Kramer test, P>0.05). **E.** Proportion of elongated to normal cells of *K. ohmeri* inside (+Halo) and outside (-Halo) the white halo around *C. sinolaborantium*, as depicted in Fig. 3A. **F.** The same growth areas as shown in **E.** but colony forming units (CFU) were measured to indicate *K. ohmeri* cell survival. Asterisks indicate different means for the Welch Two Sample t-test (p-value < 0.01). All error bars are standard error (n>3).

Characterization of the killer yeast *Candida sinolaborantium*. *C. sinolaborantium* was identified as a killer yeast with a broad antifungal spectrum that could inhibit 39 of the 69 yeast strains tested (Fig. 2 and S1). In contrast, the next most potent killer yeasts could only inhibit 11 strains tested. *C. sinolaborantium* was also able to cause large zones of growth inhibition in many different species of yeasts that were resistant to other killer yeasts (Fig. 2A). After several

292 days of incubation, we observed that *K. ohmeri* produced a striking white halo between a zone
293 of growth inhibition and methylene blue staining when challenged by the killer yeast *C.*
294 *sinolaborantium* (Fig. 3A). This phenotype was unique to the pairing of *C. sinolaborantium*
295 and *K. ohmeri*, and was distinct from the growth inhibition caused by the killer toxin K62 (the
296 only other known killer toxin capable of inhibiting *K. ohmeri*) (Fig. 2A). The white halo also
297 appeared to be raised from the surface of the agar plate (Fig. S2). When cells in this area (+halo)
298 were observed under a microscope, they appeared to be elongated compared to cells of *K.*
299 *ohmeri* outside of the halo (-halo) (Fig. 3A). The killer toxin (or toxins) secreted by *C.*
300 *sinolaborantium* were precipitated by ethanol and remained active when incubated at room
301 temperature, but were inactivated by heating to 60°C and 98°C (Fig. 3B). The inhibition of *K.*
302 *ohmeri* by *C. sinolaborantium* was optimal at pH 5 (Fig. 3C, Table S3), with loss of killing at
303 pH >5.5. The optimal temperature for killing *K. ohmeri* by *C. sinolaborantium* was 20°C. Using
304 *C. castelli* as a sensitive lawn indicated a wider optimum temperature (17-25°C) and pH (3.5-
305 5.0) (Fig. 3D, Table S3 and S4). In both cases the there was no killer activity at 35°C (Fig. 3C
306 and 3D, Table S4). Further analysis of the white halo of *K. ohmeri* revealed an 8-fold increase
307 in cell elongation in the white halos (+halo) when compared to untreated cultures of *K. ohmeri*
308 (-halo) (Fig. 3E and Table S5). Cells of *K. ohmeri* from the white halo or untreated culture were
309 seeded on agar to measure viability by colony-forming units. Cells isolated from the white
310 halos showed a 2.1-fold reduction in colony-forming units compared to *K. ohmeri* isolated
311 away from halos (Fig. 3F and Table S6). Ultrafiltration of culture media was used to determine
312 the approximate molecular weight of the antifungal molecules produced by *C.*
313 *sinolaborantium*. Antifungal activity was observed for fractions that enriched molecules >100
314 kDa and >30 kDa. Raw filtrates and concentrated ethanol-precipitated fractions were used to
315 challenge a panel of yeasts previously shown to be susceptible to toxins produced by *C.*
316 *sinolaborantium* (Fig. 2). The spent culture medium showed less antifungal activity compared
317 to the precipitated medium, with the latter capable of inhibiting 21/29 susceptible yeasts that
318 were inhibited in killer assays on agar (Fig. S3). Antifungal activities were similar before and
319 after passage through a filter with a molecular weight cut-off (MWCO) of 100 kDa and were
320 mostly retained in the MWCO 30 kDa filter. Only weak antifungal activity was detectable for
321 the fraction that passed through the MWCO 30 kDa filter (Fig. S3). The appearance of white
322 halos was observed using fractions captured by filters with MWCO 100 kDa and MWCO 30
323 kDa when tested against *K. ohmeri* but not with MWCO 5 kDa. Together, these data show that
324 *C. sinolaborantium* is a killer yeast with a broad spectrum of antifungal activities, with similar
325 temperature and pH optima of other previously described yeast killer toxins, but with the ability

326 to induce cell elongation in *K. ohmeri*. Fractions from ultrafiltration are consistent with the
327 antifungal activities of *C. sinolaborantium,* suggesting either the production of multiple
328 chromosomally encoded killer toxins with similar antifungal properties or perhaps large
329 oligomers or complexes of a single >30 kDa killer toxin.
330
331 **Ksino: a novel killer toxin produced by *C. sinolaborantium* with structural homology to**
332 **the Klus killer toxin.** To determine the gene or genes responsible for killer toxin production
333 by *C. sinolaborantium*, the genome sequence of the yeast was determined (Table S7). The
334 resulting 11.21 Mb assembly resulted in a BUSCO completeness (Complete and single-copy
335 BUSCOs) of around 98% using the saccharomycetes_odb10 dataset (Seppey et al., 2019), with
336 GC content of 49%, an N50 of 155,979 bp, and a total of 5,951 protein-coding genes (Table
337 S7). To identify genome-encoded killer toxins in the *C. sinolaborantium* proteome, BLASTp
338 was performed using a database of known killer toxins from yeasts (Table S8). This approach
339 identified 12 toxin-like candidates, all with a sequence alignment length greater than 100 amino
340 acids and an identity of at least 24% compared to any known killer toxin (Table S9). One *C.*
341 *sinolaborantium* protein had a 28% identity and 42% similarity over an alignment length of
342 151 amino acids with the *S. cerevisiae* killer toxin Klus and was named Ksino (Genbank
343 Accession: XAT76252) (Table S9) (Rodríguez-Cousiño et al. 2011).
344

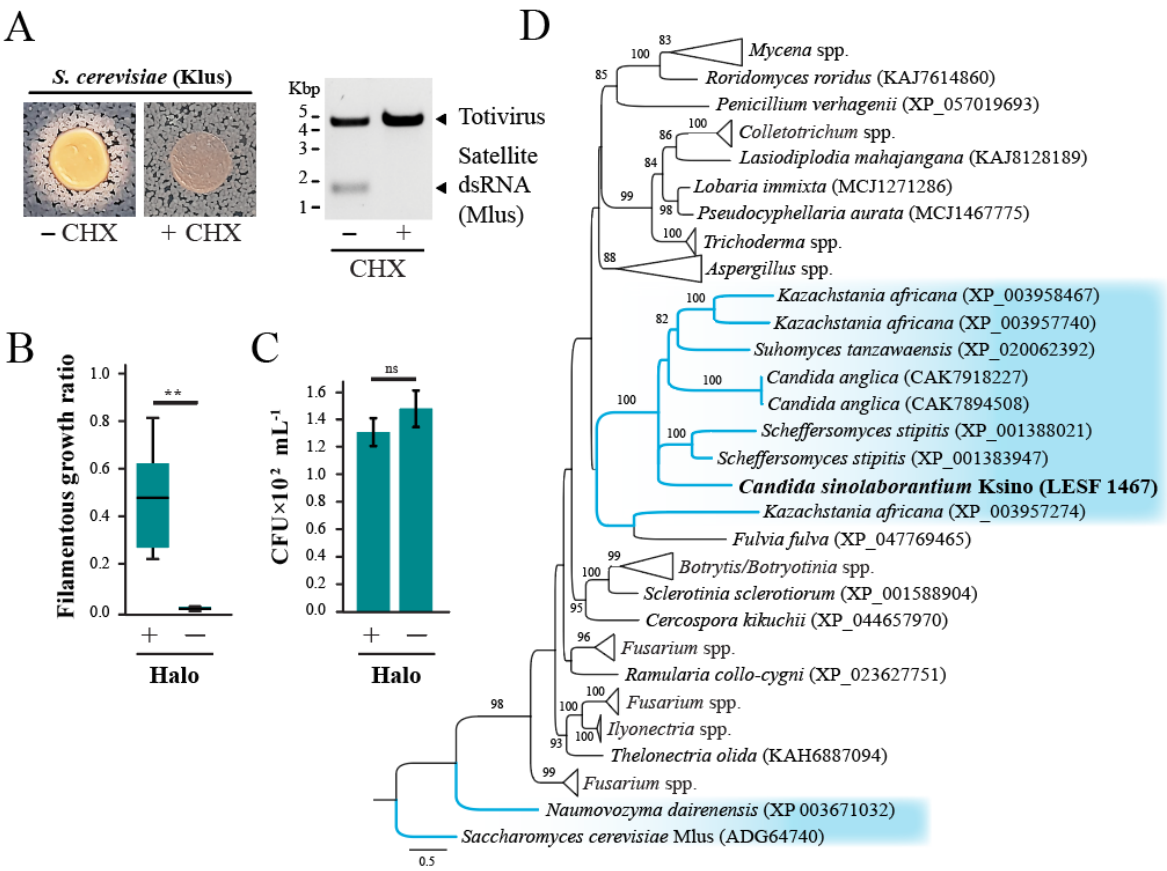

FIG 4. Ksino from *C. sinolaborantium* defines a novel family of killer toxins. **A.** The phenotypes associated with the co-culture of the Klus-encoding killer yeast *S. cerevisiae* strain DSM-70459 with *K. ohmeri* (+Mlus). Treatment with cycloheximide (CHX) causes the loss of the Mlus satellite (-Mlus) and the loss of the white halo phenotype. The ratio of **B.** elongated and **C.** viable *K. ohmeri* cells in the white halo around Klus-producing *S. cerevisiae* (+Halo) and in axenic culture (-Halo). Asterisks indicate different means for Welch Two Sample t-test (p-value <0.01), ns = not significant. **D.** A maximum likelihood phylogeny of Ksino homologs identified in diverse fungi. The Ksino from *C. sinolaborantium* is highlighted in bold, and all Saccharomycotina yeasts are highlighted in blue. The dsRNA-encoded killer toxin Klus is represented as an outgroup. Bootstrap values higher than 70 are shown. All error bars are standard error (n>3).

The sequence similarity between Ksino and Klus prompted a more detailed investigation into whether these killer toxins share similar antifungal properties. Although we had previously failed to detect growth inhibition of *K. ohmeri* by *S. cerevisiae* killer toxin Klus (Fig. 3), we noted the appearance of white halos instead of a zone of growth inhibition or methylene blue staining after prolonged co-culture (Fig. 4A). The appearance of white halos was similar to those produced by *C. sinolaborantium* and was dependent on the presence of the Mlus satellite dsRNA that encodes the Klus killer toxin gene (Fig. 4A). Analysis of the cells within the white halo found a significant proportion of elongated cells, as previously observed upon exposure of *K. ohmeri* to Ksino (Fig. 4B). However, unlike the Ksino halos, Klus did not cause a significant loss of cell viability (Fig. 4C).

366 To identify other possible Ksino-homologous proteins in different organisms, we
367 performed a BLASTp search across the NCBI database, resulting in 84 protein sequences from
368 various Ascomycota and Basidiomycota fungi. Ksino homologs were found in
369 *Saccharomycetes, Pichiomycetes* yeasts, and other filamentous fungi with identity and
370 alignment lengths higher than 30% and 109 amino acids, respectively (Fig. 4D and Table S11).
371 Phylogenetic analysis of homologs, with Klus as an outgroup, indicates that proteins with the
372 highest identity of Ksino (35-42% identity) were all uncharacterized genes of the
373 Saccharomycotina yeasts from the lineages of *Debaryomycetaceae* and the
374 *Saccharomycetaceae* (Fig. 4D). Saccharomycotina species with Ksino-like genes included
375 *Candida anglica*, *Kazachstania africana*, *Scheffersomyces stipitis*, and *Suhomyces*
376 *tanzawaensis*, with both *K. africana* and *S. stipitis* (Basionym: *Pichia stipitis*) being previously
377 reported as killer yeasts (Antunes and Aguiar, 2012; Fredericks et al. 2021). Filamentous fungi
378 encode the majority of Ksino homologs (75 out of 84), including species belonging to the
379 genera *Fusarium*, *Mycena*, and *Aspergillus* (Fig. 4D and Table S11), known as plant and human
380 pathogens (*Fusarium* spp.), saprophytic and biotrophic plant associated fungi (*Mycena* spp.),
381 and fungi species that are ubiquitous in the environment (*Aspergillus* spp.) (Summerell et al.
382 2010, Harder et al. 2023; Thoen et al. 2020; Houbraken et al. 2020; Jurjevic et al. 2012;
383 Peterson et al. 2001).
384
385 The Ksino open reading frame was determined to be 202 amino acids long, comparable
386 to Klus at 242 amino acids. Linear representation of the secondary structure revealed a similar
387 pattern of alpha helices and beta sheets (Fig. 5A; Fig. S5). There was also evidence of potential
388 post-translational modification sites, including N-terminal signal sequence cleavage sites
389 predicted by psipred (Buchan et al., 2013) and dibasic motifs (i.e., KR) in the unstructured
390 region before helix 1 (Fig. S5). Dibasic motifs in killer toxins are known to be proteolytically
391 cleaved by the Golgi-specific protease Kex2 (Julius et al., 1984). As Ksino has no sequence
392 homology to a protein of known structure, AlphaFold2 was used to generate tertiary structure
393 models of Ksino and Klus (Jumper et al., 2021). Ksino and Klus had global LDDT scores of
394 63.6 and 65.1, respectively, and per residue, LDDT was greater than 80 in regions of secondary
395 structure for both proteins (Fig. 5A and S5). Molecular dynamics simulation improved the bond
396 angles of the alphafold model to Ramachandran favored regions in models of Ksino (77% to
397 91%) and Klus (73% to 89%) (Table S10, Fig. S6). Ksino and Klus simulations reached a stable
398 RMSD of around 1.6 nm after approximately 20 ns of simulation (Fig. S6). Molprobity scores,
399 analogous to structure resolution, were determined to be 1.54 for Ksino and 1.86 for Klus

(Studer et al., 2019). Overlay of the final energy-minimized structures of Ksino with Klus compared to the original AlphaFold2 models yielded an RMSD of 2.6 Å (Fig. 5B). The predicted organization of the Ksino structure consists of a discontinuous five-stranded antiparallel beta-sheet packed against a pair of antiparallel alpha helices (Fig. 5B and S5). The tertiary structure of Klus follows the same overall organization but with one less beta-turn. Ksino has eight cysteine residues, compared to the seven in Klus (Fig. S5). The predicted structures have three intramolecular disulfide bonds. In Ksino, C105-C127 is positioned to crosslink the C-terminus of helix 1 to the beta-sheet 2, similar to C141-C162 in Klus (Fig. S5). The remaining predicted disulfide bonds are unique to both structural models (Fig. S5). These simulations collectively suggest that the Klus and Ksino proteins share significant structural homology despite having low amino acid identity.

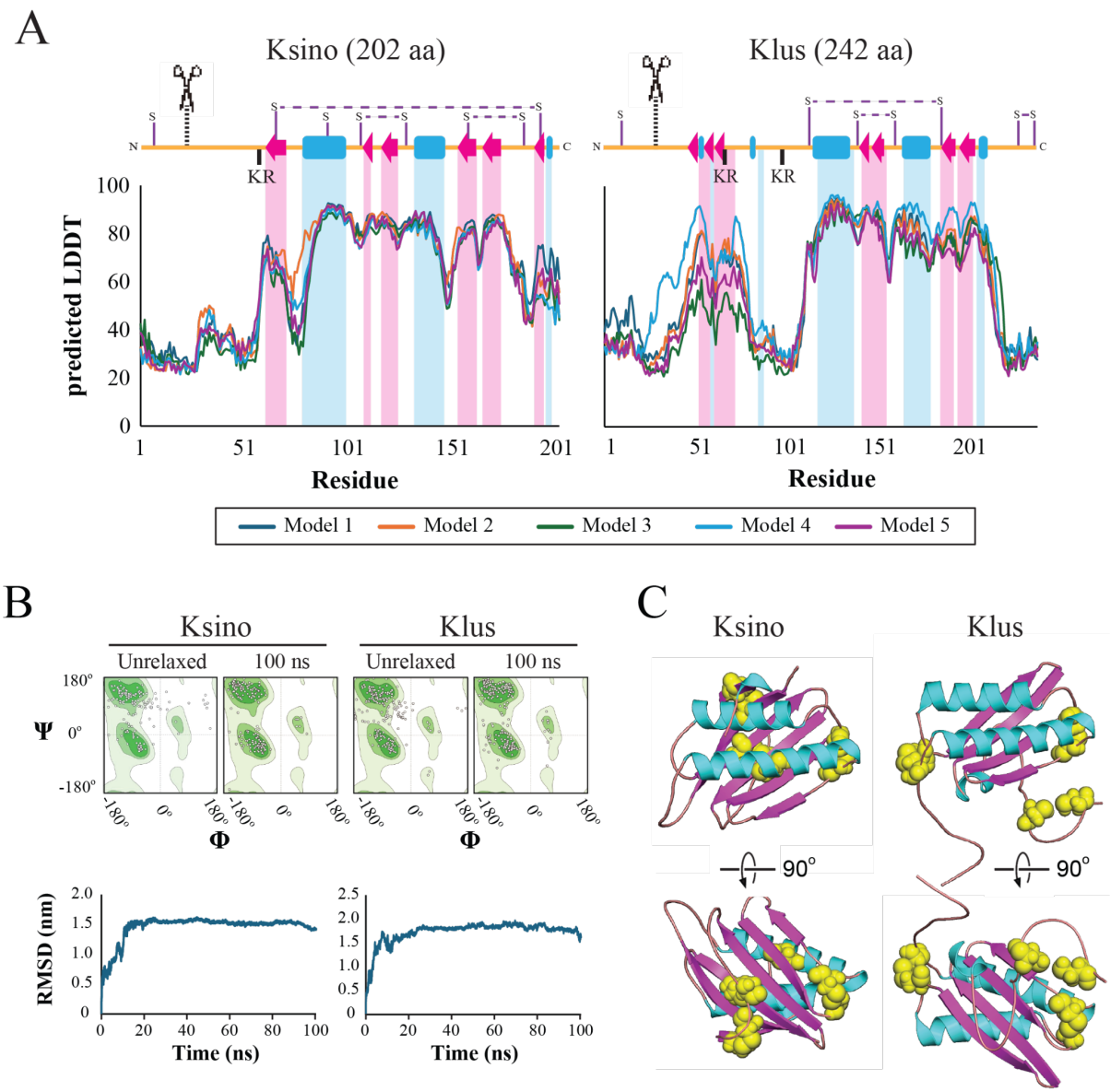

Figure 5. Molecular modeling of Ksino indicates structural homology to Klus. pLDDT confidence per residue and predicted disulfide bond arrangement of AlphaFold2 models of Ksino and Klus. A. Secondary structure representations aligned with per-residue pLDDT (predicted local distance difference test) scores from AlphaFold2. Alpha helices are represented as blue rectangles, beta sheets as red arrows, and unstructured regions as orange lines. Predicted disulfide linkages are indicated as horizontal dashed lines. Scissors with vertical dashed lines represent predicted signal sequence cleavage sites. B. Ramachandran plots of general residues (non-proline/glycine) generated by SWISS structure assessment tool demonstrating improved Ramachandran favored after performing 100 ns simulation. The unrelaxed structure represents AlphaFold2's raw output (Ramachandran et al., 1963). **B.** Full protein RMSD over 100 ns molecular dynamics simulation. GROMACS was used to generate alignments of each snapshot back to the structure at 0 ns. C. Ksino and Klus AlphaFold2 models with cysteine residues highlighted as yellow spheres to illustrate predicted disulfide linkage arrangement. The cartoon helices and beta sheets are colored to match panel A.

427 The molecular weight of Ksino was predicted to be 21.5 kDa, which appeared to be
428 smaller than the predicted molecular weight determined by ultrafiltration (Figure S3). To
429 determine if Ksino was was expressed by *C. sinolaborantium*, total RNA was extracted from
430 laboratory cultured yeast cells in order to assay for the presence of Ksion transcript by reverse
431 transcriptase PCR (RT-PCR). This approach was successful in detecting the presence of Ksino
432 RNA transcripts (Figure S4). To confirm that Ksino is an active killer toxin, the gene was
433 amplified by PCR and cloned into an *S. cerevisiae* expression vector under the control of a
434 galactose-inducible promoter. *C. sinolaborantium* belongs to the Serinales order and uses the
435 CUG codon to encode serine (Groenewald et al 2023; Krassowski et al., 2018). Ksino has one
436 CUG codon that will introduce a leucine at position 186 when expressed by *S. cerevisiae*. This
437 mutation is predicted to have a small destabilizing effect on folding compared to the wild type
438 based on FoldX 5.0 and molecular dynamics simulation (estimated $\Delta\Delta G_{Folding}$ = 1.0 kcal/mol)
439 (Fig. 5). Therefore, residue 186 was recoded for serine in *S. cerevisiae* (L186S). When the
440 strains were grown on dextrose or galactose containing media, no growth inhibition of *K.*
441 *ohmeri* was observed during co-culture with a laboratory strain of *S. cerevisiae* transformed
442 with the wild type or L186S expression vectors (Fig. SXX). However, challenging the strain
443 *C. castelli* Y-17070 with Ksino wild type or L186S on galactose triggered large zones of
444 inhibition and methylene blue staining, indicating that Ksino is a novel killer toxin (Figure 6A).
445 Growth of *S. cerevisiae* under different temperatures and pH identified that Ksino has an
446 optimum antifungal activity at pH4-4.5 (Figure 6B and Table S13) and 20-25ºC (Figure 6C
447 and Table S14), which was narrower than the killer phenotype of *C. sinolaborantium* (Figure
448 3). The inability of Ksino expressed by *S. cerevisiae* to prevent the growth of *K. ohmeri* and
449 differences in the optimal conditions for antifungal activity on *C. castelli*, indicated that Ksino
450 may be one of many antifungal molecules produced by *C. sinolaborantium*, or that expression
451 of Ksino by *S. cerevisiae* alters the toxins spectrum of activity (Fig. 4F and S8).

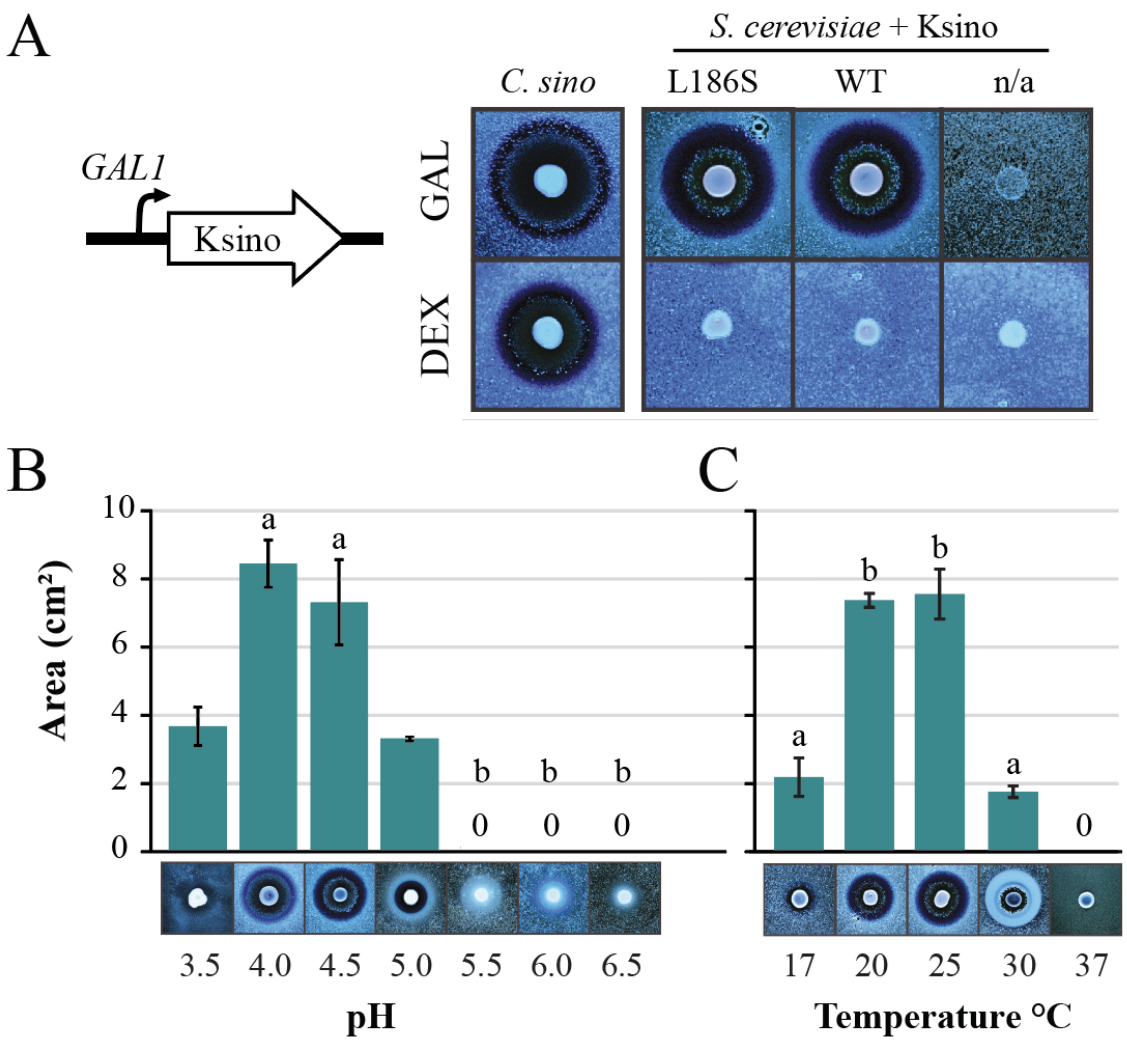

Figure 6. Ksino is an antifungal killer toxin when expressed by *S. cerevisiae*. A. Recombinant expression of Ksino (L186S) by *S. cerevisiae* using galactose induction with a lawn of *C. castelli* Y-17070 (pH 4.5). Dextrose was used as a non-induced control. n/a indicates an empty vector negative expression control. Zones of growth inhibition were compared to the killer phenotype of *C. sinolaborantium*. B. Killer yeast activity under different **B**. pH and **C**. temperature conditions as measured by zone of growth inhibition and methylene blue staining. Representative images of the killer phenotype are displayed under each histogram. The means were significantly heterogeneous (one-way anova, $P<0.01$) for both the pH and temperatures tested. Means with the same letter are not significantly different from each other (Tukey–Kramer test, $P>0.05$). All error bars are standard error (n=3).

3. Discussion

The large number of killer yeasts in fungicultures suggests they might play a role in attine ant fungus gardens by suppressing fungal competitors or allelopathy effects on complex dynamics of microbial interactions. Different studies have revealed that yeasts are abundant in attine ant environments that likely represent differences in the foraging composition and

substrate preparation behaviors observed among the different fungicultures (Bizarria Jr. et al., 2022, de Fine Licht and Boomsma, 2010; Ronque et al., 2019). Yeasts from fungus gardens of the leaf-cutting ant *Atta texana* were observed to suppress the growth of fungal garden contaminants, especially *Escovopsis* and *Syncephalastrum* (Rodrigues et al. 2009). These antifungal properties were hypothesized to contribute to fungal garden "immunity," whereby the resident fungi within a fungiculture prevent invasion by other fungal species. This would require interplay between the cleaning behaviors of attine ants in their gardens to remove unwanted fungi and other microbial interactions within attine ant colonies, i.e., allelopathy. Our study indicates that fungus gardens of attine ants harbor killer yeasts with similar prevalence to other surveys (Philliskirk and Young, 1975; Pieczynska et al., 2013; Starmer et al., 1987; Stumm et al., 1977; Trindade et al. 2002; Wojcik and Kordowska-Wiater, 2015; Abranches et al. 1997, Abranches et al. 1998). This expands the previous findings regarding the prevalence of killer yeasts in laboratory-reared attine ant colonies of *Atta sexdens* (Carreiro et al., 2002). Moreover, the prevalence of killer yeasts among the different ant species, such as *Mycetophylax* aff. *auritus* (43%, eight nests sampled) and *Mycetomoellerius tucumanus* (46%, four nests sampled) were considerably higher than in other surveyed fungicultures.

Killer yeasts from attine ant colonies were more likely to inhibit the growth of susceptible strains from different fungicultures. This supports previous observations of killer and non-killer yeast interactions whereby local selective pressure for killer toxin resistance allows the coexistence of killer and non-killer yeasts in a given niche (Starmer et al. 1987; Ganter and Starmer, 1992, Abranches et al. 1997, Trindade et al. 2002). The susceptibility of yeast populations that have never been exposed to a specific killer toxin would greatly depend on the standing genetic variation (perhaps in the cell wall and membrane toxin receptors) among different lineages of yeasts dictated by the population's evolutionary history. Our findings support the hypothesis that yeasts contribute to fungal garden "immunity" since killer yeasts are expected to prevent the invasion of other fungal species into the fungus garden. The coexistence of killer and non-killer yeast species could be an outcome of microhabitats in the spatially structured environment of the fungus garden, which may harbor different populations of yeasts and allow the colonization by killer yeasts (Giometto et al. 2021, Wloch-Salamon et al. 2008).

Saccharomycotina yeast species isolated in attine ant gardens have been previously found to secrete killer toxins. Among the yeast species, the ability to produce toxins was

observed for *Diutina catenulata* (Basionym: *Candida catenulata*; Stopiglia et al., 2014; Fuentefria et al., 2007), *Kodamaea ohmeri* (Synonym: *Pichia ohmeri*; Fuentefria et al., 2006, Fuentefria et al., 2008; Coelho et al., 2009), *Schwanniomyces vanrijiae* (Madbouly et al., 2020), and *Wickerhamomyces ciferrii* (Basionym: *Hansenula ciferrii*; Nomoto et al., 1984). The exception was *Jamesozyma spencerorum* (Synonym: *Kazachstania spencerorum* nom. inv.), which, to our knowledge, is the first report of a killer phenotype displayed by this species, although toxin production has been previously reported in the genus, specifically *K. africana*, *K. exigua* and *K. unispora* (Perez et al., 2016; Stopiglia et al., 2014; Fredericks et al., 2021). These yeast species have also been identified in substrates that are commonly foraged or associated with attine ants, including plants (*Schwanniomyces vanrijiae*, Madbouly et al., 2020; *Kodamaea ohmeri*, Fuentefria et al., 2006), insects and their environments (*Candida blattae*, Nguyen et al., 2007; *Candida sinolaborantium*, Suh et al., 2005; Guamán-Burneo et al., 2015; *Schwanniomyces vanrijiae*, Maksimova et al., 2016; *Kodamaea ohmeri*, Benda et al., 2008; Amos et al., 2019; Suh and Blackwell, 2005), and soil (*Jamesozyma spencerorum*, Synonym : *Kazachstania spencerorum* nom. inv.; Vaughan-Martini et al., 1995; Kurtzman, 2003; Kurtzman and Robnett, 2003; Liu et al., 2024).

Importantly, killer yeast species appear to be unique between colonies of the same ant species (Bizarria Jr. et al., 2023). This observed diversity could be due to the foraging behavior of ants, whereby sampling of the surrounding environment would introduce different fungal species to the fungiculture of the same species of ants in different geographical locations (Bizarria Jr. et al., 2023). However, despite the potential role of killer yeasts in garden immunity, whether the occurrence of killer yeasts in a fungiculture is acquired by chance, inherited from the environment, or inherited during garden propagation remains unknown (Bizarria Jr. et al., 2022). Niche construction by the fungal cultivar species could also play a role in yeast diversity in the fungus garden environment or by other features such as the pH of the fungus garden. Interestingly, the pH observed in the different fungus gardens (pH 5.1-5.4) is consistent with the optimal antifungal activities of *C. sinolaborantium* (pH 3.5-5.0) and Ksino (pH 4.0-4.5). However, the association between killer yeasts and fungicultures still requires robust empirical evidence to reject the stochastic nature of killer yeast colonization. Future yeast isolation will provide new directions to clarify whether killer yeast occurrence is modulated by ant foraging choice or fungus garden features such as pH and fungal cultivar species.

536 Our survey of the encoding elements of killer toxins indicated that the 180 isolated
537 strains of Saccharomycotina yeasts were devoid of cytoplasmic killer toxin-encoding elements
538 such as dsRNA satellites and dsDNA linear plasmids. The frequency of dsRNA elements
539 associated with *Saccharomyces* yeasts has been observed to range from 10% to 51% in wild
540 and domesticated strains (Pieczynska et al., 2013; Crabtree et al., 2023). It is expected that
541 more of these genetic elements will be found in other Saccharomycotina lineages, given their
542 discovery in non-*Saccharomyces* yeasts and the frequency of genome-integrated molecular
543 fossils of plasmid and virus sequences in different lineages (Frank and Wolfe, 2009; Liu et al.,
544 2010; Satwika et al., 2012; Myers et al., 2020; Villan Larios, et al. 2023; Taylor and Bruenn,
545 2009, Lee et al., 2022). Most of the yeast isolated from fungicultures belong to the Serinales,
546 where the CUG codon is translated into serine instead of leucine in the universal genetic code
547 (Groenewald et al 2023). The rewiring of the fungal genetic code has been suggested to prevent
548 the invasion of viruses and plasmids by stopping the faithful translation of viral proteins
549 (Krassowski et al., 2018). Alternatively, RNAi might also contribute to limiting viral infections
550 in these yeasts, even though, in some cases, yeast lineages maintain viruses that suppress RNAi
551 (Drinnenberg et al., 2009; Drinnenberg et al., 2011; Lee et al., 2022; Segers et al., 2006; Segers
552 et al., 2007; Rodriguez Coy et al., 2022). RNAi and genome recoding could be possible reasons
553 for the absence of cytoplasmic elements in the yeasts associated with attine ant fungiculture.
554 However, this still requires a more in-depth investigation to exclude the stochastic nature of
555 virus acquisition by fungi and sampling biases.
556
557 The lack of extrachromosomal elements in killer yeasts associated with attine ant
558 fungiculture suggests that killer toxin genes are genome-encoded. Our survey indicates that the
559 killer toxins from different Saccharomycotina lineages associated with fungus gardens differ
560 in their spectrum of antifungal activity from canonical *Saccharomyces* killer toxins (K1, K2,
561 K28, etc.). In particular, toxins secreted by *Candida sinolaborantium* had the broadest activity,
562 including toward infectious human pathogens (e.g., *Candida albicans*, *C. glabrata*, and *C.*
563 *auris*). A unique response to the killer activity of *C. sinolaborantium* was also observed in *K.*
564 *ohmeri*, where cells exposed to the killer yeast grew as filaments. Usually, dimorphism in
565 yeasts has been demonstrated to be triggered by nitrogen starvation (Gimeno et al., 1992),
566 different carbon sources, and temperature (Rupert and Rusche, 2022). However, to our
567 knowledge, this is the first case of this phenotype associated with exposure to a killer yeast . The
568 broad spectrum antifungal activities of *C. sinolaborantium* and the ability to fractionate
569 antifungal activities by ultrafiltration indicates the likely presence of multiple unidentified

570 chromosomally encoded toxins. After determining the genomic sequence of *C.*
571 *sinolaborantium*, the new killer toxin Ksino was discovered due to its sequence homology to
572 the canonical *Saccharomyces* killer toxin Klus. However, the killer activity of *C.*
573 *sinolaborantium* was not fully reproduced when Ksino was heterologously expressed by *S.*
574 *cerevisiae* and was unable to inhibit or cause filamentouse growth in *K. ohmeri*. Instead robust
575 growth inhibition was only observed after challenging *C. castelli.* These data also supports the
576 expression of multiple killer toxins by *C. sinolaborantium* or that ectopic heterologous
577 expression by *S. cerevisiae* is inadequate due to potential deficiencies in extracellular export,
578 maturation, or Ksino's innate toxicity.
579
580 Many proteins from different Ascomycete and Basidiomycete fungi lineages were
581 identified in our search for Ksino-like proteins, including filamentous fungi and yeast (from
582 Saccharomycetes and Pichiomycetes). The Ksino-like proteins from yeasts of the
583 Saccharomycotina subphylum (*Candida anglica*, *Kazachstania africana*, *Scheffersomyces*
584 *stipitis*, and *Suhomyces tanzawaensis*) share a closer evolutionary origin to Ksino and therefore
585 might represent bonafide killer toxins. Despite our approach to identifying killer toxins being
586 limited by primary sequence similarity to known toxins, it has successfully identified Ksino.
587 This combination of genome sequencing, sequence homology searches, and structural
588 modeling could be used more widely on the many killer yeasts that are devoid of cytoplasmic
589 extrachromosomal elements to identify new killer toxins (Boynton, 2019; Crabtree et al. 2023).
590
591 In summary, this study demonstrates that (i) Fungus gardens of attine ants can harbor
592 killer yeasts, an underappreciated environment for killer yeasts. (ii) DsRNA and dsDNA
593 extrachromosomal elements are lacking from yeasts associated with attine ant fungicultures.
594 (iii) Genome mining can discover new chromosomally encoded killer toxins, specifically Ksino
595 secreted by *Candida sinolaborantium*. (iv) Ksino has sequence and structural homology to the
596 *Saccharomyces* killer toxin Klus and is a member of a new family of killer toxins in
597 Ascomycete and Basidiomycete fungi.
598

599 **Funding sources**

600 This work was supported by Fundação de Amparo à Pesquisa do Estado de São Paulo
601 (FAPESP) [scholarships No. 2019/24412–2 and 2021/09980-4] to RBJ and [grant No.

2019/03746–0] to AR. The authors also thank the Conselho Nacional de Desenvolvimento Científico e Tecnológico (CNPq) for a research fellowship [grant No. 305269/2018–6] to AR and a scholarship [No. 142396/2019–2] to RBJ. This work was supported by the Institute for Modeling Collaboration and Innovation at the University of Idaho (National Institutes of Health grant P20GM104420), Idaho Institutional Development Awards Network of Biomedical Research Excellence (INBRE) Program Core Technology Access Grant (NIH Grant Nos. P20GM103408), and National Science Foundation Grant No. 2143405. The content is solely the responsibility of the authors and does not necessarily represent the official views of these funding agencies.

Data Availability

Data supporting the results in the paper are available in the Supplementary Material. The GenBank accession number for the Open reading frames of the Ksino killer toxin of *Candida sinolaborantium* LESF 1467 is PP790515. The sequenced genome of *Candida sinolaborantium* can be accessed through BioProject PRJNA916362, BioSample SAMN32422847, Assembly JAQRFW000000000. The raw sequence reads are also available through the NCBI Sequence Read Archive (SRR23081998). Gene prediction and annotation are provided in https://figshare.com/s/1f31cd262fc9de969d38 (10.6084/m9.figshare.25895278).

Acknowledgments

We would like to thank Conselho de Gestão do Patrimônio Genético (CGEn) for providing permits for access to genetic heritage: #AE012D8, #A877F11 and #AA39A6D. We also thank Amanda Viana and Luciana Simão Carneiro for preparing and preserving yeast cultures. We also would like to thank the ARS Culture Collection (NRRL), Westerdijk Fungal Biodiversity Institute (WI-KNAW), and Dr. Roland Klassen for providing yeast cultures used in this study. We also thank Dr. Primrose Boynton for the critical reading of this manuscript. Photos of ants in Fig. 1 were accessed from "www.antweb.org": CASENT0173791 *Acromyrmex coronatus* (Photographer: April Nobile); CASENT0909391 *Mycetomoellerius tucumanus* (Photographer: Will Ericson); CASENT0901666 *Mycetophylax auritus*

632 (Photographer: Ryan Perry); CASENT0173988 *Mycocepurus goeldii* (Photographer: April
633 Nobile); CASENT0922040 *Apterostigma goniodes* (Photographer: Michele Esposito).

634

635 **Authors' contributions**

636 RB wrote the manuscript supervised by PAR and with inputs from AR, JWC, and MY;
637 RB conducted cross-interaction killer assays and dsRNA extractions. JWC performed protein
638 structure predictions and analysis. TJB conducted cross-interactions with pathogenic yeasts.
639 RACS performed genome assemblage and annotation. SAC performed killer assays for Ksino
640 characterization. SAC performed microscopic evaluations and killer assays. RB and RTT
641 performed dsDNA extractions. NF and MJD performed genome sequencing. PAR and AR
642 supervised and obtained funding for the project. AR is responsible for permit applications. All
643 authors discussed and reviewed the manuscript and approved the final version.

644

645 **Supplementary figures**

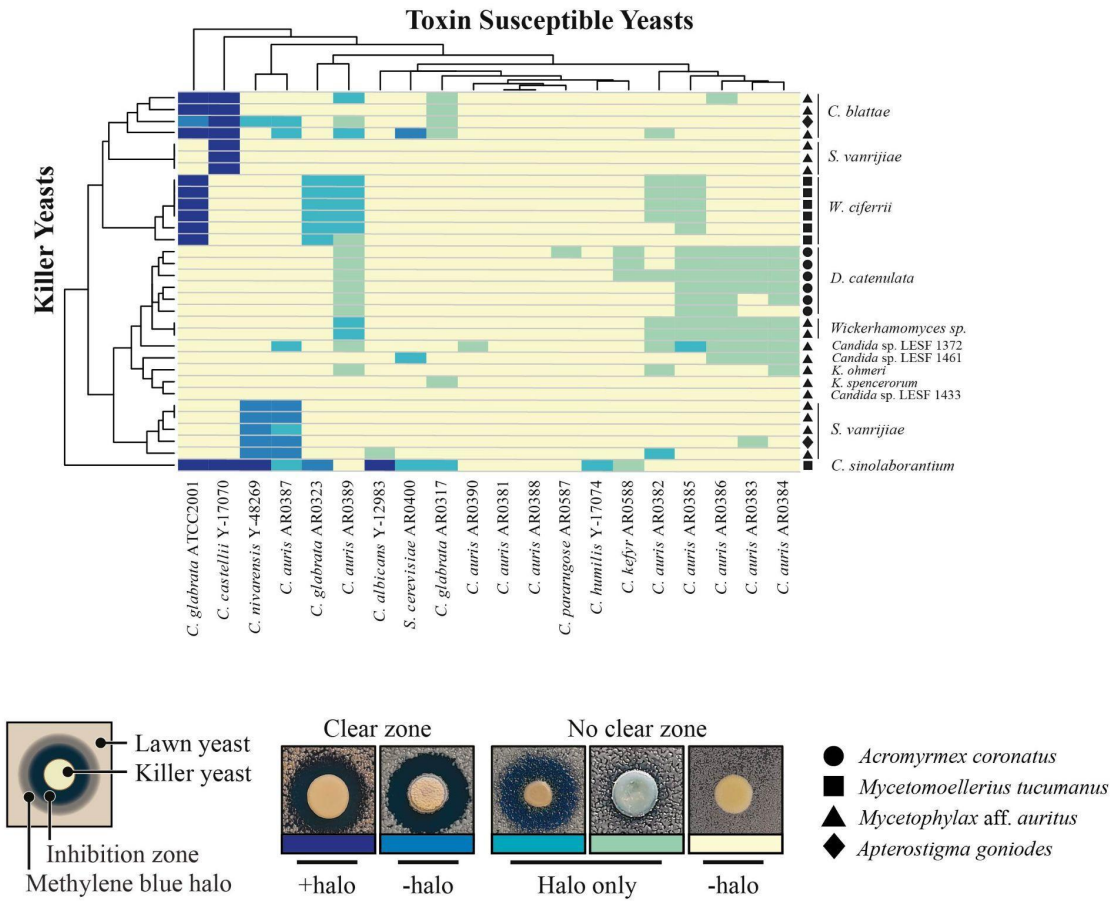

FIG S1. Killer yeasts from attine ant gardens can inhibit the growth of opportunistic human pathogens. A heatmap showing interactions between killer yeasts associated with attine ants and opportunistic human pathogens. Origins of the ant-associated killer yeasts; *Acromyrmex coronatus* (circle); *Mycetomoellerius tucumanus* (square); *Mycetophylax* aff. *auritus* (triangle), *Apterostigma goniodes* (diamond). Killer toxin activity was qualitatively assessed based on the presence and size of growth inhibition zones and/or methylene blue staining around killer yeasts as diagrammed. Darker colors on the heatmap represent a more prominent killer phenotype, with yellow indicating no observable killer phenotype. Clusters on the dendrograms connecting individual killers or susceptible yeasts indicate similar susceptibilities to killer toxins or antifungal activities. Darker colors on the cluster diagram represent a more prominent killer phenotype, with yellow indicating no observable killer phenotype.

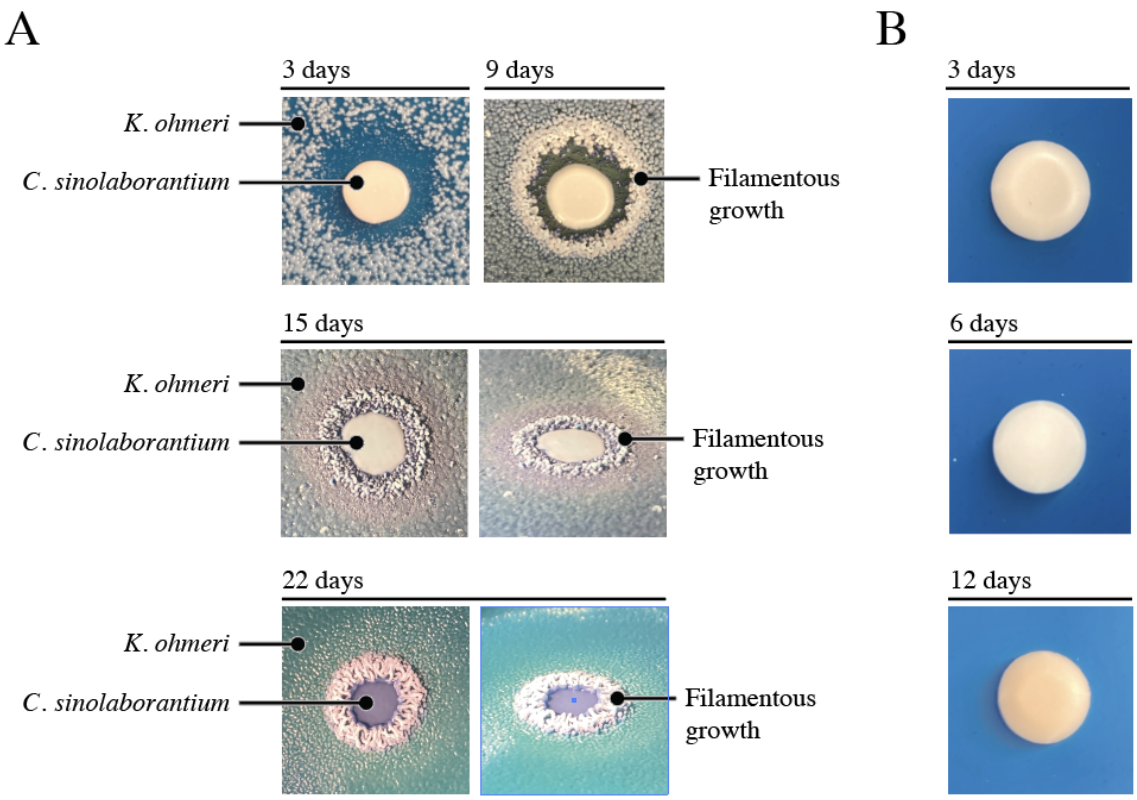

FIG S2. Elongated growth of *K. ohmeri* after coculture with the killer yeast *C. sinolaborantium*. A. Representative images showing the interaction between *K. ohmeri* and the killer yeast *C. sinolaborantium* on YPD agar. After extended incubation times at ~22ºC (15 - 22 days), vertical growth from the surface of the agar was observed. B. Elongated growth phenotypes are not observed when *C. sinolaborantium* is grown in isolation on agar.

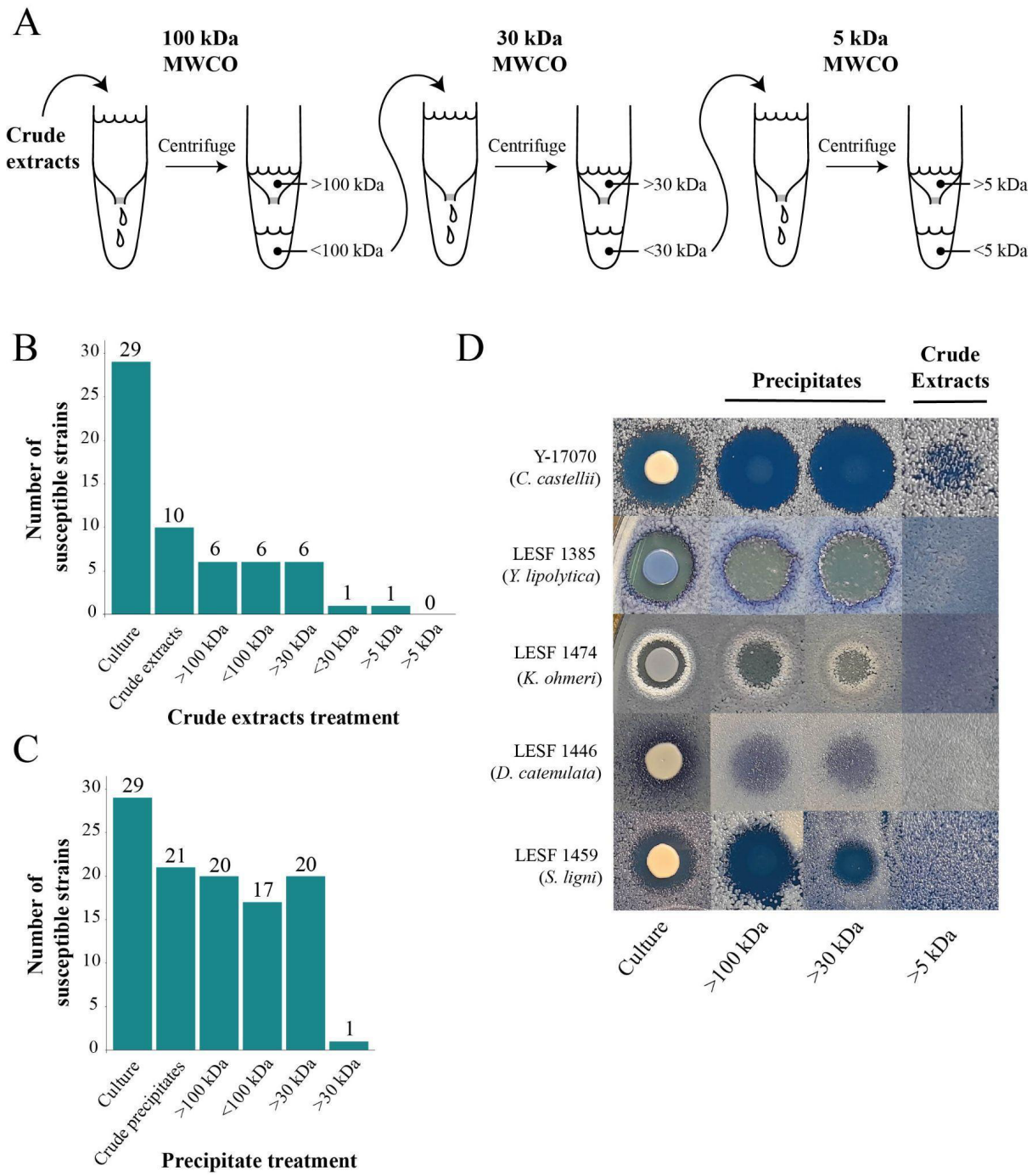

FIG S3. Antifungal activities exhibited by fractionated media after growth of *Candida sinolaborantium*. A. The workflow demonstrates the ultrafiltration of YPD-spent growth media to obtain fractions of antifungal molecules. Crude extracts were processed by ultrafiltration with molecular weight cut-off (MWCO) filters of 100 kDa, 30 kDa, and 5 kDa. The resulting protein preparations were used to challenge susceptible yeasts before (>) and after (<) ultrafiltration. Fractions were used **B.** before or **C.** after ethanol-precipitation **D.** Phenotypic examples of antifungal activity detectable in different fractions against representative susceptible yeast species.

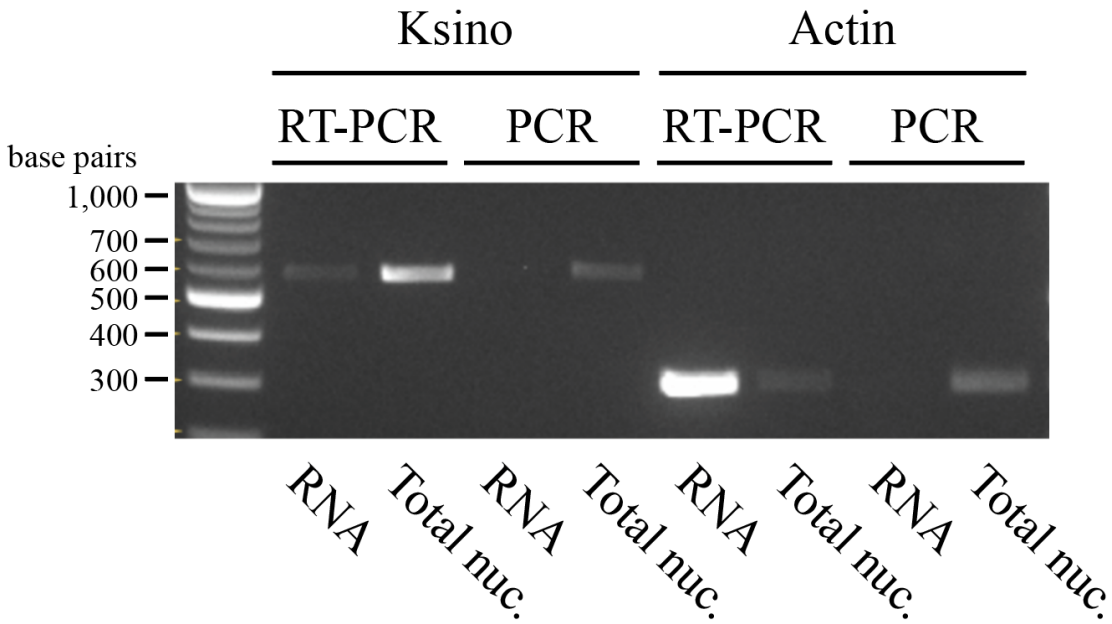

671

672 **FIG S4. Detection of Ksino expression by RT-PCR.** XXXXXX

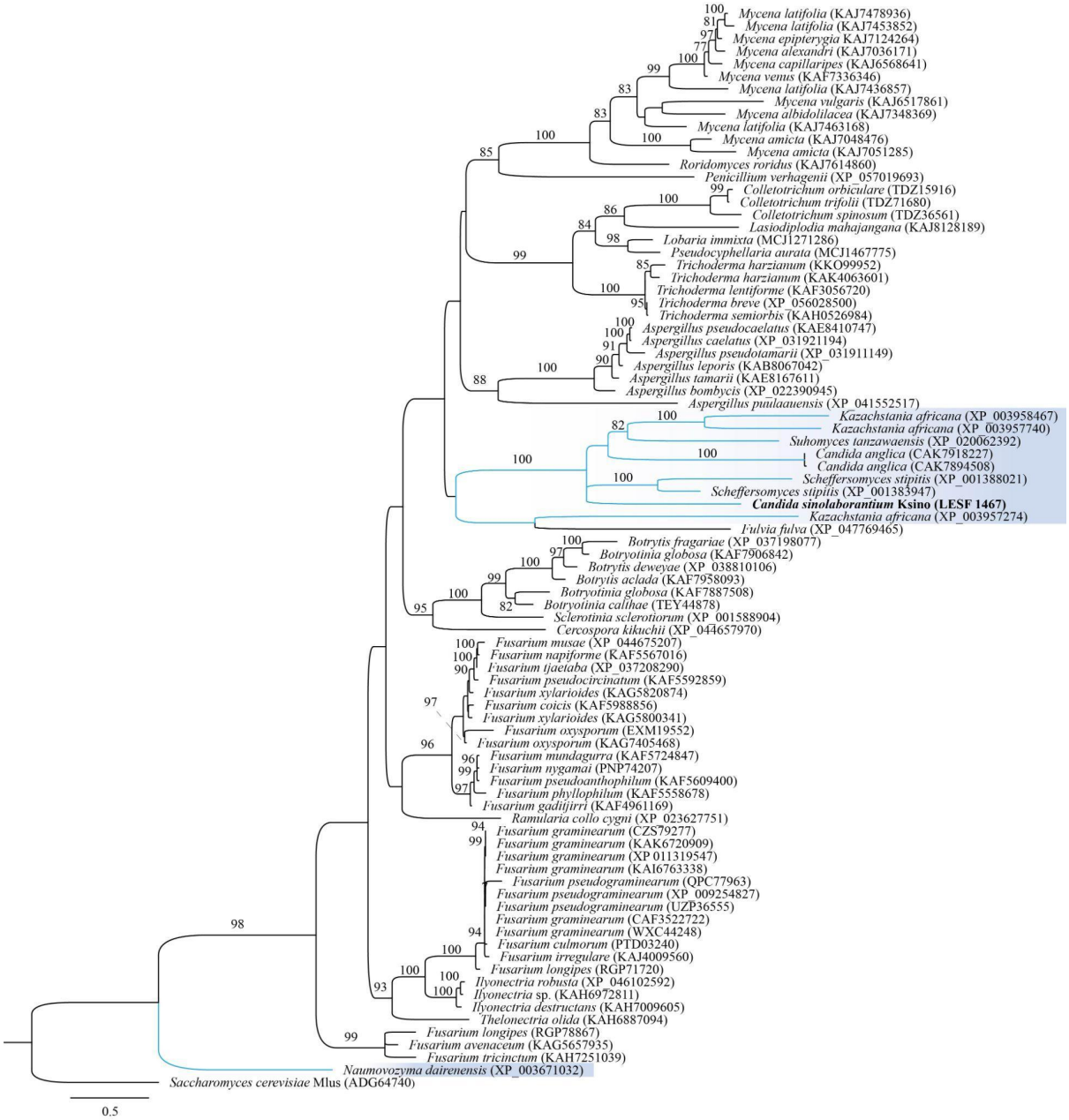

FIG S5. Phylogeny of Ksino homologs identified in diverse fungi. The Ksino-encoding yeast *C. sinolaborantium* is highlighted in bold, and Saccharomycotina in blue. The tree was inferred with maximum likelihood criteria, and numbers on branches are ultrafast bootstrap support values (only values higher than 70 are shown). The dsRNA-encoded killer toxin Klus is represented as an outgroup.

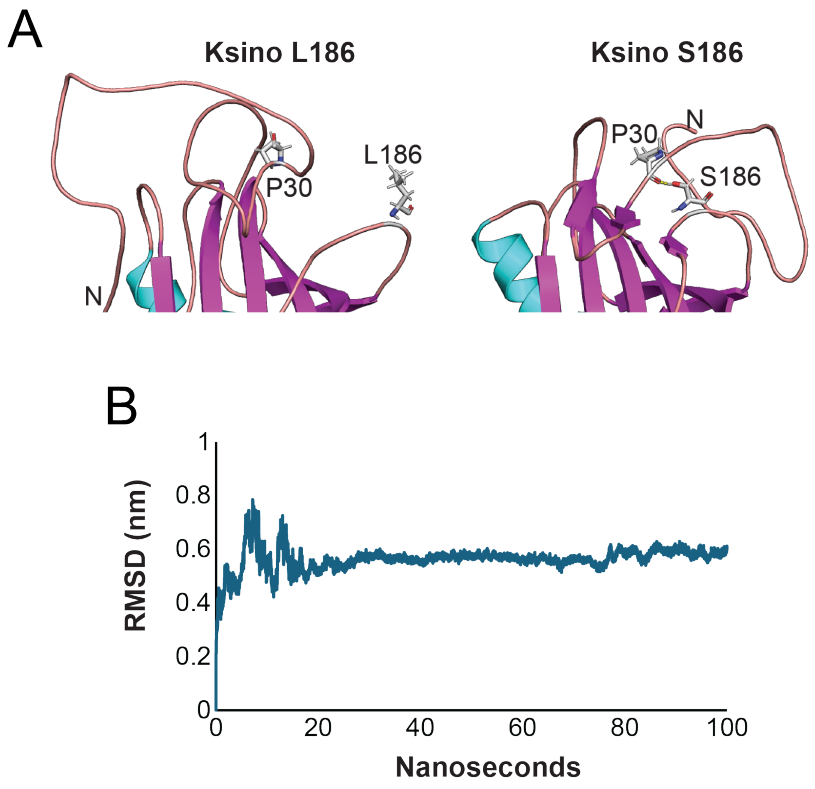

FIG S6. Computational predictions of protein stability with leucine and serine at position 186 in Ksino. A. AlphaFold2 models of Ksino wild type S186 and mutant L186 after 100 ns of molecular dynamics simulation. Residues 186 and P30 are shown as sticks. P30 forms a hydrogen bond (1.6 Å) with the hydroxyl of S186 but is too distant to create this bond in L186. FoldX 5.0 analysis revealed a $\Delta\Delta G_{Folding}$ of 1.0 kcal/mol for L186S. **B.** 100 ns MD simulation of Ksino L186 AlphaFold2 model. Unlike wild type and Klus, the RMSD stabilizes around 0.55 nm.

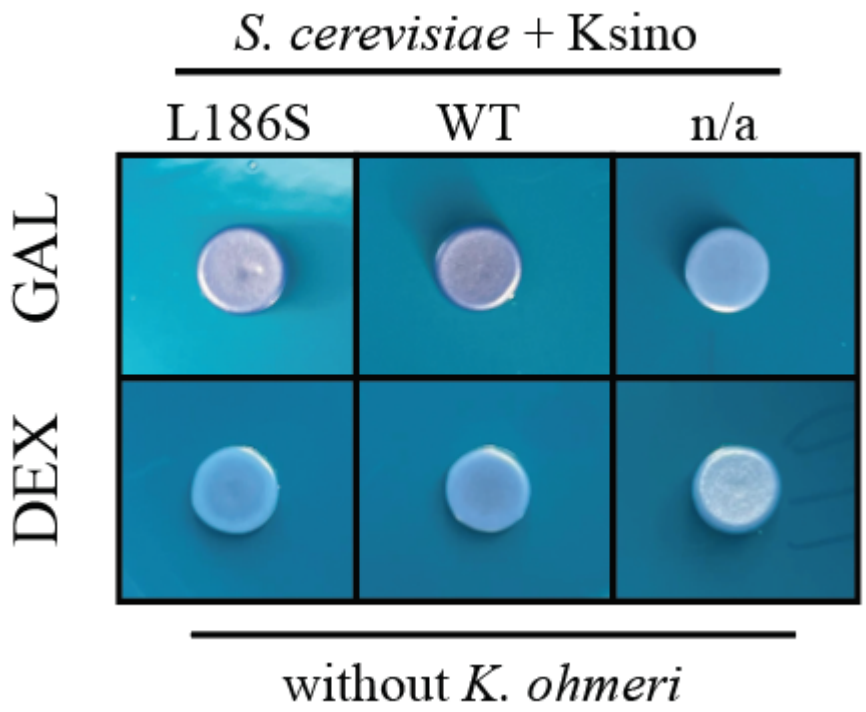

FIG S7. Recombinant expression of Ksino does not cause a white coloration of *S. cerevisiae*. Recombinant expression of Ksino by *S. cerevisiae* using galactose induction without a lawn of *K. ohmeri*. Dextrose was used as a non-induced control. n/a indicates an empty vector negative expression control.

Supplementary Tables

Table S1. Strains and species of yeasts used in the current study.

Table S2. The effect of isolation source on killer yeasts activity.

Table S3. The effect of pH on the growth inhibition of *Kodamaea ohmeri* LESF 1474 and *C. castelli* by *Candida sinolaborantium* LESF 1467

Table S4. The effect of temperature on the growth inhibition of *Kodamaea ohmeri* LESF 1474 and *C. castelli* by *Candida sinolaborantium* LESF 1467.

Table S5. The ratio between elongated and yeast morphology of *Kodamaea ohmeri* LESF 1474 cells challenged with killer toxins.

Table S6. Cell survival of *Kodamaea ohmeri* LESF 1474 cells against killer toxins.

704 **Table S7.** Statistics of the assembly, prediction, and annotation of the *Candida*
705 *sinolaborantium* LESF1467 genome.

706 **Table S8.** Killer toxins were used as queries for the BLASTp search of the *Candida*
707 *sinolaborantium* LESF1467 genome.

708 **Table S9.** Blastp hits of killer toxins towards *Candida sinolaborantium* LESF1467 genome.

709 **Table S10.** SWISS-MODEL structure assessment scores of Ksino top unrelaxed model and
710 Klus top unrelaxed model compared to models after 100 ns of molecular dynamics simulation.
711 Global pLDDT score is also included in the last row.

712 **Table S11.** Statistics of Blastp hits of Ksino homologs.

713 **Table S12.** Nucleotide sequences used in phylogenetic analysis of yeast species delimitation.
714
715 **Table S13.** The effect of pH on the growth inhibition of *Kodamaea ohmeri* LESF 1474 and
716 *Candida castyelli* by Ksino expressed by *S. cerevisiae*.
717
718 **Table S14.** The effect of temperature on the growth inhibition of *Kodamaea ohmeri* LESF
719 1474 and *Candida castyelli* by Ksino expressed by *S. cerevisiae*.

720 **Table S15.** Yeasts used in killer assays as susceptible or killer positive standards.

721

722 **Supplementary files**

723 **File S1** - All killer assay data.
724
725 **File S2 -** PDB coordinates for the molecular models of Ksino and Klus.
726
727
728 ## 4. Materials and Methods

729

730 ### 4.1. Yeast source and phylogenetic analysis

731

732 To investigate the prevalence of killer yeast in the fungus garden of attine ants, a
733 representative collection of 180 yeasts previously characterized by Bizarria Jr. et al. (2023) was
734 examined (Table S1). Briefly, yeasts were obtained by fungus garden suspension in saline
735 solution (0.85% NaCl) supplemented with 0.05% Tween 80. Suspensions were ten-fold diluted
736 and surface spread on nutrient media (Yeast-malt agar and Sabouraud dextrose agar,
737 supplemented with 150 µg mL^{-1} chloramphenicol, and pH adjusted to 4.5; details in Bizarria

738 Jr. et al. 2023). Yeast characterization involved microsatellite amplification analysis (MSP-
739 PCR; Meyer et al. 1993) and sequencing of the D1/D2 region of the large subunit (LSU)
740 ribosomal RNA gene (Kurtzman and Robnett, 1998). Our selection of the 180
741 *Saccharomycotina* yeasts spanned from fungus gardens of the leaf-cutting ant *Acromyrmex*
742 *coronatus* (n = 91), the non-leaf-cutting ant *Mycetomoellerius tucumanus* (n = 13), the lower
743 attines *Mycetophylax* aff. *auritus* (n = 42), and *Mycocepurus goeldii* (n = 25), which cultivate
744 *Agaricaceae* fungi; and *Apterostigma goniodes* (n = 9), which cultivates *Pterulaceae* fungi.
745 To assess the phylogenetic relationship between the yeast strains, we performed a
746 phylogenetic analysis with representative species and their closest relatives (the accession
747 number of sequences used in phylogenetic analysis is listed in Table S12). Sequences were
748 aligned with MAFFT v.7. (Katoh et al. 2019), and nucleotide substitution models were
749 generated using the Bayesian information criterion (BIC) by the standard model generation in
750 IQ-TREE2. SYM+FQ+I+G4 was selected as the nucleotide substitution model. Maximum
751 likelihood (ML) phylogenetic trees were reconstructed with ultrafast bootstrap in IQTREE2
752 (Nguyen et al. 2015), with 10,000 replicates for ultrafast bootstrap (tree completed after 262
753 iterations, LogL: -14973.244). The final trees were edited in FigTree v.1.4.3 (Rambaut, 2016).
754
755 **4.2. Killer yeast assays**
756
757 Killer assays were performed to confirm killer toxin production by yeasts, as described
758 in Crabtree et al. (2019). The 180 yeast strains were seeded onto YPD 4.6 dextrose "killer
759 assay" agar plates (yeast extract 10 g L^{-1}, peptone 20 g L^{-1}, dextrose 20 g L^{-1}, sodium citrate
760 29.9 g L^{-1}, supplemented with 0.003% w/v methylene blue, and pH adjusted to 4.6 with HCl),
761 seeded 10^5 cells mL^{-1} with one of the 49 selected yeast susceptible strains (i.e. from fungus
762 gardens and sources not related to attine ant environment, Table S13). Nine *Saccharomyces*
763 spp. strains that encode known toxins were used as positive controls for killer toxin productio,
764 including K1, K1L, K21, K2, K28, K45, K62, K74, and Klus (Table S13). Yeasts were also
765 evaluated using 20 pathogenic yeasts as susceptible strains (Table S13). Toxin production was
766 recorded after five days of incubation at room temperature, either by an inhibition zone or a
767 methylene blue stain of susceptible strains. Killer activity severity was scored following
768 Fredericks et al. (2021) by zone of inhibition with or without methylene blue halo or by strong
769 or weak methylene blue halo without inhibition. We applied heatmaps to visualize the species
770 interactions, employing the function heatmap.2 from the gplots package, with the default

771 configuration for dendrogram display (Warnes et al., 2024). To evaluate the effect of the yeast
772 sources (i.e., same or different fungicultures or sites) on killer toxin activity (i.e., killed or non-
773 killed). We selected 9,000 interactions (toward 50 strains that showed susceptibility to killer
774 toxins) and analyzed them with Pearson's Chi-squared test. All yeasts used in killer assays are
775 listed in Table S15.
776
777 **4.3. Extraction of dsRNA encoding elements**
778
779 To determine if the yeast strains host dsRNA elements, we extracted the dsRNA
780 elements from all yeast strains following Okada et al. (2015), with modifications as stipulated
781 in Crabtree et al. (2019). The K1 killer yeast *S. cerevisiae* BJH001 was used as a positive
782 control for all assays. Specifically, yeast cultures were grown in yeast-peptone-dextrose broth
783 (YPD: yeast extract 10 g L^{-1}, peptone 20 g L^{-1}, dextrose 20 g L^{-1}), centrifuged at 3000 × g
784 for 5 min, and the broth was removed by aspiration. Cells were resuspended in water,
785 centrifuged at 8,000 × g, and aspirated. A total of 450 µL of 2× sodium chloride-Tris-EDTA
786 buffer (STE: 200 mM NaCl; 20 mM Tris-HCl, pH 8.0; 30 mM EDTA) and 0.5 µL β-
787 mercaptoethanol were added, and cells were disrupted in a cell disruptor (Digital Disruptor
788 Genie, Scientific Industries) for 3 min at 3000 rpm. Then, 50 µL of 10% (w/v) sodium dodecyl
789 sulfate (SDS) solution and 350 µL phenol–chloroform–isoamyl alcohol (25:24:1) were added
790 to crude extracts, which were homogenized and centrifuged at 10,000 × g for 5 min. Then, 500
791 µL of supernatant was mixed with absolute ethanol (5:1), and the final volume of 600 µL was
792 transferred to cellulose columns (i.e., 0.05 g cellulose D in a 0.6 mL tube bottom punctured
793 and placed in collecting tubes).
794 Column tubes were centrifuged at 10,000 × g for 30 seconds, and the flow-through was
795 discarded. Then, 350 µL of wash buffer (1× STE containing 16% v/v EtOH) was added to the
796 column, and the tubes were centrifuged at 10,000 × g for 30 seconds, followed by the flow-
797 through discard. Columns were transferred to a collecting tube, adding 350 µL of 1× STE, and
798 tubes were centrifuged at 10,000 × g for 30 seconds. The eluted fraction was recovered, and 1
799 mL of absolute ethanol with 40 µL of 3 M aqueous sodium acetate (pH 5.2) was added. Tubes
800 were inverted ten times and centrifuged at 20,000 × g for 15 min. The ethanol mix was aspirated
801 without disturbing the precipitated pellet, which was then air-dried and dissolved in 15 µL of
802 molecular-grade water. The presence of dsRNAs was examined (loading 5 µL of each sample)
803 by 0.8% TAE agarose gel electrophoresis, stained with ethidium bromide, at 130 v for 30 min

804 in 1% TAE buffer. As a molecular weight reference, a 1 kb DNA ladder was used. The
805 *Saccharomyces cerevisiae* strain YJM1307, known to host dsRNA totivirus and satellites, was
806 used as positive control.
807
808 **4.4. Extraction of dsDNA linear plasmid**
809
810 To determine if dsDNA linear plasmids encode the killer toxins, we extracted the
811 dsDNA elements from positive killer yeast, *Kluyveromyces lactis* AWJ137 with the linear
812 DNA plasmids pGKL2 (13.5 kb) and pGKL1 (8.9 kb) and *Pichia acaciae* NRRL Y-18665 with
813 the linear plasmids pPac1-1 (12.6 kb) and pPac1-2 (6.8 kb) (Worsham and Bolen, 1990; Gietz
814 et al., 1995). Cultures were grown in YPD overnight, 200 µL were centrifuged at 3000 × g for
815 5 min, and the broth was removed by aspiration. Yeast cells were resuspended in 10 µL
816 Zymolase solution (5% of 50 mM Tris-HCl, pH 8; 10% of 5 mM EDTA, and 85% water) and
817 7.2 µL of 10 mg mL^{-1} of Zymolase (United States Biological Life Sciences, Swampscott, MA),
818 and the suspension was incubated at 30°C for 1 h. After incubation, 1 µL of 10% SDS and 3
819 µL of proteinase K (New England Biolabs, Ipswich, MA) were added to the suspension,
820 followed by an incubation of 1 h at 65°C. After incubation, 5 µL of loading dye was added,
821 and the suspension was centrifuged at 3000 × g for 5 min. The presence of dsDNA plasmids
822 was examined (loading 10 µL of each sample) by 0.6% TAE agarose gel electrophoresis,
823 stained with ethidium bromide, at 130 v for 1 h in 1% TAE buffer.
824
825 **4.5. Toxin precipitation and killer toxin activity at different temperatures and**
826 **pH**
827
828 To investigate the stability of the toxins produced by *C. sinolaborantium* LESF 1467,
829 the isolate extracts on YPD medium (pH 4.6) were filtered, mixed with 1:1 absolute ethanol,
830 centrifuged at 20,000 × g for 20 min, followed by supernatant aspiration and suspension in 10
831 µL of YPD (pH 4.6). To confirm the killer activity of the precipitates, 4 µL of the suspended
832 proteins were used in killer assays against *Kodamaea ohmeri* LESF 1474. To evaluate the
833 thermostability, the precipitated toxins were screened in killer assays incubating at room
834 temperature or heat-inactivated at 60ºC and 98°C for 2 min. For quantitative analysis of killer
835 toxin expression, 2 µl of 10^8 cells mL^{-1} were plated onto susceptible lawns.The killer activity
836 was also evaluated for activity at different pHs, adjusting the pH to 3.5, 4, 4.5, 5, 5.5, and 6
837 with HCl 12N, and at various temperatures, incubating at 17, 20, 25, 30, and 35°C. The area of

838 activity on killer assays (i.e., zone of inhibition and cell differentiation of the lawn strain) was
839 measured in cm^2 after four days with ImageJ 1.53t (Schneider et al., 2012). Since the area data
840 do not satisfy the assumptions of parametric tests, we analyzed variance with Kruskal-Wallis
841 followed by the Wilcoxon rank sum test with Bonferroni correction as a post-hoc for pairwise
842 multiple comparisons. Analyses were performed using the software RStudio v. 2023.12.0.369
843 (POSIT TEAM, 2023), and R v. 4.3.2 (R CORE TEAM, 2023). Figures were prepared using
844 ggplot2 (Wickham, 2016).
845
846 **4.6. Production of elongated cells by *Kodamaea ohmeri* against killer toxins**
847
848 We observed that the yeast *K. ohmeri* LESF 1474 produces elongated cells in the
849 presence of *C. sinolaborantium* toxins and their precipitates. We suspended the cells in the
850 white and raised zones of killer assays and on axenic cultures in 1× PBS. Cell morphology was
851 checked under a microscope (Zeiss Primo Star iLED) by counting budding (2 to 17 × 10^6 cells
852 mL^{-1}) and elongated cells (2 to 15 × 10^5 cells mL^{-1}) with a Neubauer chamber. Cell survival
853 was evaluated by adjusting the suspensions to 10^3 cells mL^{-1} and seeding 100 µL in YPD.
854 Colony-forming units (CFU) were counted after three days of incubation at room temperature.
855 A similar elongated cell phenotype was observed in the presence of *S. cerevisiae* DSM-70459,
856 which secretes the known killer toxin Klus (encoded by dsRNA elements). Microscopic and
857 survival evaluations were also conducted in the presence of *S. cerevisiae* DSM-70459, as
858 described above. To confirm that the elongated cell phenotype is related to the presence of the
859 dsRNA satellites, dsRNA satellites were cured from *S. cerevisiae* by growing on a YPD
860 medium supplemented with 5.0 µM cycloheximide. Loss of killer toxin production and the loss
861 of dsRNAs were assayed as described above. The ratio between normal and elongated cells
862 was compared between *K. ohmeri* in the white halo around *C. sinolaborantium* and *S.*
863 *cerevisiae* DSM-70459 with axenic cultures surrounding the halo, with ten independent
864 replicates. The data was checked for the assumption of parametric tests (performing Shapiro-
865 Wilk and Bartlett tests, respectively, for normality and homogeneity of variances). The ratio
866 data in both treatments, towards *C. sinolaborantium* and *S. cerevisiae* DSM-70459, were found
867 not to satisfy the assumptions of equal variance (Bartlett test, df = 1, p-value < 0.001), so we
868 conducted the Welch Two Sample t-test to compare means between treatments. The same
869 procedure was performed for cell survival data towards *C. sinolaborantium*, which also did not
870 satisfy the assumptions of equal variance (Bartlett's K-squared = 4.16, df = 1, p-value = 0.04).
871 Cell survival data towards *S. cerevisiae* DSM-70459 satisfied the assumptions for parametric

872 tests (Bartlett's K-squared = 0.52, df = 1, p-value = 0.47; Shapiro-Wilk p-value > 0.05), so we
873 conducted the Two Sample t-test to compare means between treatments.
874
875 **4.7. Genomic DNA extraction, sequencing, and annotation**
876
877 To extract genomic DNA from *C. sinolaborantium*, the yeast was grown in YPD broth;
878 cells were recovered by centrifugation (3000 × g for 5 min), washed, and suspended in 500 µL
879 TE buffer (10 mM Tris-Cl; 0.1 mM EDTA, pH 8). Recovered cells were transferred to a
880 microtube, centrifugation as previously described, and the supernatant was removed. The pellet
881 was disrupted by vortexing. Cells were suspended in a lysis buffer (2% Triton X-100, 1% SDS,
882 100 mM NaCl, 10 mM Tris-HCl, pH 8, 1 mM EDTA pH 8) with approximately 300 µL of
883 glass beads. A volume of 200 µL of phenol-chloroform-isoamyl alcohol solution was added,
884 and the sample was vortex for 3 min at 3000 rpm (Disruptor Genie), followed by the addition
885 of 200 µL of TE buffer and centrifugation for 5 min at 21000 × g. The upper layer was
886 transferred to a new microtube and mixed by inversion with 1 mL of absolute ethanol. The tube
887 was centrifuged for 3 min at 21000 × g, the supernatant removed, and the pellet suspended in
888 400 µL of TE buffer. Then, 30 µL of DNAse-free RNAse A was added, and the solution was
889 mixed and incubated for 5 min at 37°C. The DNA was precipitated by adding 10 µL of 4 M
890 ammonium acetate and 1 mL of absolute ethanol, mixing by inversion, and centrifuging for 3
891 min at 21000 × g. The supernatant was discarded and the pellet was dried for approximately
892 20 min at room temperature. Genomic DNA was suspended in 100 µL of TE buffer and stored
893 at -20°C.
894 The genome was sequenced by Illumina NextSeq 550 using the paired-end method.
895 Libraries were created with the Illumina DNA Prep kit for WGS
896 (https://www.illumina.com/products/by-type/sequencing-kits/library-prep-kits/nextera-dna-
897 flex.html). The initial quality analysis and cleaning steps were performed with fastp v. 0.20.1
898 (CHEN et al., 2018). The genome was assembled with SPAdes v. 3.15.5 (GUREVICH et al.,
899 2013) with multiple k-mers (21, 31, 41, 51, 61, 71, and 81). The blobtools v. 3.5.2 software
900 (LAETSCH; BLAXTER, 2017) was used to check contaminants. Briefly, Blastn 2.13.0+
901 (ALTSCHUL et al., 1990) was used to search for structures across the entire NCBI nt database;
902 minimap2 v. 2.24-r1122 (LI, 2018) and samtools v.1.13 (LI et al., 2009) were used to obtain
903 sequencing coverage. The blobtools visualization was used to ascertain the results. The rDNA
904 and ITS regions were annotated with ITSx v. 1.3 (BENGTSSON-PALME et al., 2013), which
905 was compared to an amplicon previously submitted to NCBI for this isolate (accession:

906 ON493969) as part of the contamination verification steps. Final assembly statistics were
907 obtained with QUAST v. 5.2.0 (BANKEVICH et al., 2012). Completeness was checked using
908 BUSCO v. 5.4.4 (SEPPEY et al., 2019) with the saccharomycetes_odb10 dataset (2,137
909 BUSCOs). The genetic prediction was performed using Braker v. 2.1.6 (BRŮNA et al., 2021)
910 [which includes Augustus v. 3.4.0 (STANKE; MORGENSTERN, 2005), ProtHint v. 2.6.0 and
911 GeneMark-ES v. 4.71 (LOMSADZE et al. 2005)] with OrthoDB v. 10 methods
912 (KRIVENTSEVA et al., 2019). InterProScan v. 5.60 (Jones et al., 2014) was used for
913 functional annotation of predicted proteins.
914
915 **4.8. Genome mining for toxin-encoding regions**
916
917 To identify toxin-encoding chromosomal regions, a search using proteins predicted
918 from whole genome sequencing was performed with BLASTP 2.9.0, using a protein sequence
919 database of known killer toxins. Results with query/hit alignments greater than 100 were
920 selected. An open reading frame similar to the Klus toxin (28% identity, with 151 aa alignment
921 length and an e-value of $1.56E^{-05}$) was found and selected for further analysis. Polymerase
922 chain reactions (PCR) were performed to amplify the region of interest using primers designed
923 with Primer3 software. 4.1.0 (https://primer3.ut.ee/). The primers were designed to target Ksino
924 untranslated regions (961F: 5'-TTAACGACTTTCGTCTTCGCTATCC-3' and 961R: 5'-
925 ATTGAGATCAGGTGGCCTGTGTAGC-3') followed by nested-PCR to amplify the open
926 reading frame using the previous PCR product as the template (961NF: 5'-
927 CGATCACCTAGCCCAAAATGC-3' and 961NR: 5'-AAAGTGTTGGCCAAGGACACG-
928 3'). Both of the amplification reactions used Phusion high fidelity master mix (New England
929 Biolabs, Ipswich, MA) with the amplification conditions of 98°C for 3 min, 30 cycles at 98°C
930 for 30 s, 63°C for 30 s, 72°C for 30 s, and a final extension step at 72°C for 5 min. Amplicons
931 were sequenced to confirm the identity of the region of interest.
932
933 **4.9. Prediction of tertiary structure and comparative analysis of proteins**
934
935 After confirming the genomic coding region of Ksino was the correct size using PCR,
936 the sequence was used to predict protein structure via the AlphaFold2 software (Jumper et al.,
937 2021) with default parameters. The B factor columns of each unrelaxed structure were used to
938 create per residue pLDDT graphs. Secondary structure was assigned using PyMol to create a
939 linear representation of the protein and aligned to per residue graphs. The top-scoring relaxed

940 model from AlphaFold2 was used for molecular dynamics simulation using the GROMACS
941 package (Spoel et al., 2005). Briefly, the system was set up using the AMBER99SB-ILDN
942 force field with TIP3P water, a dodecahedral box with 1.0 nm padding, and 0.15 M NaCl. The
943 system was then subjected to energy minimization by steepest descent, followed by NVT and
944 NPT equilibration with a pressure of 1.0 atm and temperature of 300 K. Pressure and
945 temperature were maintained constant using arrinello-Rahman with isotropic coupling and V-
946 rescale with Protein Non-protein as the coupling groups, respectively. This setup was chosen
947 to match standard cellular conditions closely: 26.85°C, 0.15 M NaCl, pH 7, and 1 atm.
948 Simulations were run for 100 ns with a 2.0 fs timestep, and snapshots were saved every 2 fs.
949 The RMSD was calculated as a function of time using the resulting trajectories. In addition, the
950 final snapshot of each trajectory was saved as a PDB structure file and compared to relaxed
951 and unrelaxed AlphaFold2 models using the SWISS structure assessment tool (Studer et al.,
952 2019).
953 FoldX was used to predict the $\Delta\Delta G_{Folding}$ of L186S (Delgado et al., 2019). Amber
954 relaxed Ksino L186 was used as the starting structure, and FoldX PDBrepair was carried out
955 six times to optimize the structure. Then, L186 in the optimized structure was mutated to every
956 other residue using PositionScan. $\Delta\Delta G_{Folding}$ was taken from the output file.
957
958 **4.10. Bioinformatic discovery of Ksino homologs in fungi**
959
960 A search for similar sequences in NCBI (https://www.ncbi.nlm.nih.gov/) was also
961 carried out with Blastp, with the results filtered by alignment length (above 109), identity
962 (above 30%), and e-value (less than 0.03). The protein sequences were aligned with MUSCLE
963 (https://www.ebi.ac.uk/jdispatcher/msa/muscle), with the alignment consisting of 86
964 sequences and 426 positions. Amino acid substitution models were generated according to the
965 Bayesian information criterion (BIC), with WAG+R4 being the chosen model. Maximum
966 likelihood (ML) phylogenetic trees were reconstructed in IQTREE2 (Nguyen et al., 2015), with
967 10,000 ultrafast bootstrap replicates (tree completed after 163 iterations, LogL: -18525.485).
968 The final trees were edited in FigTree v.1.4.3 (RAMBAUT, 2016).
969
970 **4.11. Cloning and transformation in *Escherichia coli***
971
972 To study the coding region, a "TA" terminal was added to the amplicon in a reaction
973 that included 1 µL Taq polymerase, 19 µL of PCR product, 1 µL of 10 µM dNTPs, 5 µL of 10×

974 buffer, and 24 µL of sterile ultrapure water. The reaction was incubated at 72°C for 20 min.
975 For cloning, the pCR™8/GW/TOPO™ TA Cloning kit (Invitrogen, Waltham, MA) was used,
976 adding 1 µL of amplicons with TA terminals, 0.25 µL of saline solution from the kit, and 0.25
977 µL of the pCR™8/GW/TOPO™ vector. The reaction was incubated at room temperature for 2
978 h, followed by adding 25 µL of competent *E. coli* cells (One-Shot TOP10 Competent Cells,
979 Invitrogen, Waltham, MA). The reaction was kept on ice for 30 min, followed by heat shock
980 at 42°C for 30 s and then ice bath for 2 min. Subsequently, 250 µL of Super Optimal broth
981 (SOC: 20 g L^{-1} Tryptone, 5 g L^{-1} Yeast extract, 0.58 g L^{-1} NaCl, 0.19 g L^{-1} KCl, 2, 03 g L^{-1}
982 $MgCl_2$, 1.20 g L^{-1} $MgSO_4$, and 3.6 g L^{-1} dextrose) preheated to 37°C was added, and incubated
983 at 37°C for 1 h. Then, 250 µL were plated on Luria bertani medium (LB: 10 g L^{-1} of tryptone,
984 5 g L^{-1} of yeast extract, 10 g L^{-1} of NaCl, and 15 g L^{-1} of agar) supplemented with 100 µg mL-
985 1 of spectinomycin. Plasmids were extracted using the High-Speed Mini Plasmid kit (IBI
986 Scientific, Dubuque, IA), following manufacturer recommendations.
987 Due to the transcriptional diversity of CUG-Leu codons in some yeasts (Krassowski et
988 al., 2018), the vectors containing the region of interest were subjected to targeted mutations
989 (SDM: Site-Directed Mutagenesis) in a CUG codon starting at position 556 of the DNA
990 sequence (position 186 in the protein sequence). Thus, the mutants consist of the alternatives
991 identified for CUG in other yeasts, being called L186A and L186S, with L being the original
992 amino acid, 186 the position, and "S" the mutation for Ser. To obtain the mutants, we design
993 primers targeting position 186 as follows: 961GCG: 5'-
994 CAGCTGTGGCGCGAACCATAGCGGG-3', 961TCG: 5'-
995 CAGCTGTGGCTCGAACCATAGCGGG-3' (forward), and 961SNM: 5'-
996 AGTCCCGCAGGCCAATCC-3' (reverse). Amplification reactions included 12.5 µL of
997 Phusion High Fidelity Master Mix, 1 µL 10 µM forward primer, 1 µL 10 µM reverse primer,
998 9.5 µL sterile ultrapure water, 1 µL 1:9 diluted DNA (i.e., pCR™8 plasmid with the region of
999 interest). Amplification conditions were as follows: 98°C for 30 min, 25 cycles at 98°C for 5
1000 s, 67°C for 10 s, 72°C for 50 s, and a final extension step at 72°C for 5 min. To remove the
1001 template DNA from the reaction, a Dpnl treatment was performed by mixing 22 µL of PCR
1002 product, 2 µL Dpnl, 3 µL CutSmart buffer, and 3 µL sterile ultrapure water. The reaction was
1003 incubated at 37°C for 1 day. For the addition of 5'-P and 3'-OH, we performed a PNK treatment:
1004 30 µL of the treated product, 5 µL PNK buffer, 1 µL PNK, 5 µL 10 mM ATP, 1 µL 0.1 M DTT,
1005 8 µL of sterile ultrapure water. The reactions were incubated for 30 min at 37°C and inactivated
1006 at 65°C for 10 min. The product was purified using the Monarch DNA & PCR Cleanup kit
1007 (New England Biolabs, Ipswich, MA), following the manufacturer's protocols. To re-ligate the

1008 plasmids, the following reaction was performed: 2 μL of purified product, 1 μL T4 DNA ligase,
1009 2 μL 10× binding buffer, 15 μL sterile ultrapure water. The reaction was incubated for 2 h at
1010 room temperature, and then 25 μL of competent *E. coli* cells (One-Shot TOP10 Competent
1011 Cells, Invitrogen, Waltham, MA) were added. Transformed cultures were selected in LB
1012 supplemented with 100 μg mL^{-1} spectinomycin, plasmids extracted with the High-Speed Mini
1013 Plasmid kit (IBI Scientific, Dubuque, IA), and mutations checked by sequencing (ELIM
1014 Biopharmaceuticals, Hayward, CA).
1015 The vectors were subjected to a Gateway™ recombination from the vectors in pCR8 to
1016 pAG306-GAL-ccdB. For recombination, the reaction was conducted with 0.5 μL of the source
1017 vector, 0.5 μL of the destination vector, 1 μL of sterile ultrapure water, and 0.5 μL of LR
1018 Clonase II (New England Biolabs, Ipswich, MA). The reaction was incubated for 4 h at room
1019 temperature, followed by adding 0.25 μL of Proteinase K (New England Biolabs, Ipswich, MA)
1020 and incubating at 37°C for 10 min. Finally, the *E. coli* transformation was performed as
1021 previously described, and cultures were selected in LB supplemented with 100 μg mL^{-1} of
1022 chloramphenicol and ampicillin.
1023
1024 **4.12. Transformation and heterologous expression of killer toxins**
1025 **by*Saccharomyces cerevisiae***
1026
1027 For yeast transformation, the integrative vector containing a killer toxin gene was
1028 linearized with the NcoI enzyme by cutting at the *URA3* locus, followed by inactivation of the
1029 enzyme at 65°C for 30 min. The product was purified using the Monarch DNA & PCR Cleanup
1030 kit (New England Biolabs, Ipswich, MA), following the manufacturer's recommendations. *S.*
1031 *cerevisiae* CRY1 cells were grown in YPD until an optical density of 1.3 was obtained, then
1032 the cells were washed with sterile water and suspended in 10 mL of TE buffer supplemented
1033 with 100 mM LiAc, and incubated at 30°C for 30 min under 130 rpm agitation. Cells were
1034 recovered by centrifugation at 1500 × g for 5 min at 4°C and suspended in 5 mL of ice-cold
1035 1M sorbitol, followed by centrifugation and suspended in 550 μL of ice-cold 1M sorbitol. For
1036 transformation, 80 μL of the suspended cells were added to 5 to 10 μg of the linearized plasmids
1037 and transferred to electroporation cuvettes. The cuvettes were incubated on ice for 10 min and
1038 pulsed with GenePulser (200 Ω, 1.5 kV, and 25 μF). To recover the transformed cultures, the
1039 cells were grown at 30°C for 2 days in CM medium without uracil (complete media: 2.5 g L^{-1}
1040 of the drop-out mix without uracil, 1.7 g L^{-1} of yeast nitrogen base YNB, 5 g L^{-1} ammonium
1041 sulfate, 20 g L^{-1} dextrose). For killer toxin expression was induced by overnight growth in

1042 YPGal (yeast extract 10 g L^{-1}, peptone 20 g L^{-1}, galactose 20 g L^{-1}) followed by plating on
1043 either YPD or YPGal with citrate-phosphate 29.9 g L^{-1}, supplemented with 0.003% w/v
1044 methylene blue and pH adjusted to 4.6 with HCl and 15 g L^{-1} agar seeded with 10^5 cells mL^{-1}
1045 of a susceptible lawn strain. *C. sinolaborantium* and *S. cerevisiae* CRY1 were used as positive
1046 and negative controls for killer activity, respectively.
1047

1048 **4.13. Detection of killer toxin expression by RT-PCR**

1049

1050 An overnight culture of Ksino was grown in YPD and harvested at OD600 0.9-1.2.
1051 Speroplasting was performed by incubating the harvested cells at 30°C for 30 min in buffer Y1
1052 (1M sorbitol, 0.1 M EDTA, pH 7.4, B-ME 0.1%, and 0.1% v/v zymolase 20T (10 mg/mL)).
1053 Spheroplasts were used as input for a Qiagen RNeasy procedure. The RNA quality was checked
1054 using a spectrophotometer, and 10 µg of total RNA was treated with 1 µL of DNase I
1055 (ThermoFisher Scientific) in the presence of 10 µL of DNase reaction buffer at 37°C for 10
1056 min, and then inactivated by heat at 75°C for 10 min. Transcripts encoding Ksino or actin were
1057 detected by RT-PCR (Superscript IV) following the manufacturer's instructions using the
1058 primers 5'-GGCCTTGAGATACCCCATCG-3' and
1059 5'-CCACGTGAGTAACACCGTCA-3' (for *ACT1*) and 5'-
1060 GATCTACGACAGCAGCCTAGA-3' and
1061 5'-GTGGTGTACATCGTTGACTCC-3' (for Ksino). Briefly, the RNA template is denatured
1062 with a reverse primer mix at 65°C for 5 min and incubated on ice for at least 1 min. The reverse
1063 transcription reaction mix was added to the denatured RNA and incubated for 10 minutes at
1064 55°C and then inactivated at 80°C for 10 minutes. A 20 L PCR was performed with the cycling
1065 instructions as follows (98°C for 30 s, then 30 cycles of 98°C for 10 s, 60°C for 30 s, 72°C for
1066 10 s followed by one cycle of 72°C for 5 min). PCR products were analyzed by agarose gel
1067 electrophoresis.

1068 **References**

1069 Abranches, J., Mendonça-Hagler, L. C., Hagler, A. N., Morais, P. B., Rosa, C. A. (1997). The
1070 incidence of killer activity and extracellular proteases in tropical yeast communities. **Canadian**
1071 **Journal of Microbiology**, 43(4), 328-336. doi: 10.1139/m97-046

1072

Abranches, J., Valente, P., Nóbrega, H. N., Fernandez, F. A., Mendonça-Hagler, L. C., Hagler, A. N. (1998). Yeast diversity and killer activity dispersed in fecal pellets from marsupials and rodents in a Brazilian tropical habitat mosaic. **FEMS Microbiology Ecology**, 26(1), 27-33. doi: 10.1111/j.1574-6941.1998.tb01558.x

Altschul, S. F., Gish, W., Miller, W., Myers, E. W., Lipman, D. J. (1990). Basic local alignment search tool. **Journal of molecular biology**, 215(3), 403-410. doi: 10.1016/S0022-2836(05)80360-2

Amos, B. A., Hayes, R. A., Leemon, D. M., Furlong, M. J. (2019). Small hive beetle (Coleoptera: Nitidulidae) and the yeast, *Kodamaea ohmeri*: a facultative relationship under laboratory conditions. **Journal of Economic Entomology**, 112(2), 515-524. doi: 10.1093/jee/toy378

Antunes, J., Aguiar, C. (2012). Search for killer phenotypes with potential for biological control. **Annals of microbiology**, 62, 427-433. doi: 10.1007/s13213-011-0256-z

Arcuri, S. L., Pagnocca, F. C., da Paixão Melo, W. G., Nagamoto, N. S., Komura, D. L., Rodrigues, A. (2014). Yeasts found on an ephemeral reproductive caste of the leaf-cutting ant *Atta sexdens rubropilosa*. **Antonie Van Leeuwenhoek**, 106(3), 475–487. doi: 10.1007/s10482-014-0216-2

Bankevich, A., et al. (2012). SPAdes: a new genome assembly algorithm and its applications to single-cell sequencing. **Journal of computational biology**, 19(5), 455-477. doi: 10.1089/cmb.2012.0021

Belda, I., Ruiz, J., Alonso, A., Marquina, D., Santos, A. (2017). The biology of *Pichia membranifaciens* killer toxins. **Toxins**, 9(4), 112. doi: 10.3390/toxins9040112

Benda, N. D., Boucias, D., Torto, B., Teal, P. (2008). Detection and characterization of *Kodamaea ohmeri* associated with small hive beetle *Aethina tumida* infesting honey bee hives. **Journal of Apicultural Research**, 47(3), 194-201. doi: 10.1080/00218839.2008.11101459

Bengtsson-Palme, J., et al. (2013). Improved software detection and extraction of ITS1 and ITS 2 from ribosomal ITS sequences of fungi and other eukaryotes for analysis of environmental sequencing data. **Methods in Ecology and Evolution**, 4(10), 914-919. doi: 10.1111/2041-210X.12073

Bevan, E. A., Herring, A. J., Mitchell, D. J. (1973). Preliminary characterization of two species of dsRNA in yeast and their relationship to the "killer" character. **Nature**, 245(5420), 81-86. doi: 10.1038/245081b0

Bizarria Jr, R., de Castro Pietrobon, T., Rodrigues, A. (2023). Uncovering the Yeast Communities in Fungus-Growing Ant Colonies. **Microbial Ecology**, 86(1), 624-635. doi: 10.1007/s00248-022-02099-1

Bizarria Jr, R., Pagnocca, F. C., Rodrigues, A. (2022). Yeasts in the attine ant–fungus mutualism: Diversity, functional roles, and putative biotechnological applications. **Yeast**, 39(1-2), 25-39. doi: 10.1002/yea.3667

Boynton, P. J. (2019). The ecology of killer yeasts: Interference competition in natural habitats. **Yeast**, 36(8), 473–485. doi: 10.1002/yea.3398

Branstetter, M. G., Ješovnik, A., Sosa-Calvo, J., Lloyd, M. W., Faircloth, B. C., Brady, S. G., and Schultz, T. R. (2017). Dry habitats were crucibles of domestication in the evolution of agriculture in ants. **Proceedings of the Royal Society B: Biological Sciences**, 284(1852), 20170095. doi: 10.1098/rspb.2017.0095

Brown, D. W. (2011). The KP4 killer protein gene family. **Current genetics**, 57, 51-62. doi: 10.1007/s00294-010-0326-y

Brůna, T., Hoff, K. J., Lomsadze, A., Stanke, M., Borodovsky, M. (2021). BRAKER2: automatic eukaryotic genome annotation with GeneMark-EP+ and AUGUSTUS supported by

a protein database. **NAR genomics and bioinformatics**, 3(1), lqaa108. doi: 10.1093/nargab/lqaa108

Buchan DWA, Minneci F, Nugent TCO, Bryson K, Jones DT (2013). Scalable web services for the PSIPRED Protein Analysis Workbench. **Nucleic Acids Res.** 41(W1): W349–W357. doi: 10.1093/nar/gkt381.

Buser, C. C., Jokela, J., Martin, O. Y. (2021). Scent of a killer: How could killer yeast boost its dispersal?. **Ecology and Evolution**, 11(11), 5809-5814. doi: 10.1002/ece3.7534

Bussey, H., Vernet, T., Sdicu, A. M. (1988). Mutual antagonism among killer yeasts: Competition between Kl and K2 killers and a novel cDNA-based K1-K2 killer strain of *Saccharomyces cerevisiae*. **Canadian journal of microbiology**, 34(1), 38-44. doi: 10.1139/m88-007

Buzzini, P., Martini, A. (2001). Discrimination between *Candida albicans* and other pathogenic species of the genus *Candida* by their differential sensitivities to toxins of a panel of killer yeasts. **Journal of clinical microbiology**, 39(9), 3362-3364. doi:10.1128/jcm.39.9.3362-3364.2001

Carreiro, S. C., Pagnocca, F. C., Bacci, M., Bueno, O. C., Hebling, M. J. A., Middelhoven, W. J. (2002). Occurrence of killer yeasts in leaf-cutting ant nests. **Folia Microbiologica**, 47(3), 259–262. doi: 10.1007/BF02817648

Castillo, A., Cifuentes, V. (1994). Presence of double-stranded RNA and virus-like particles in *Phaffia rhodozyma*. **Current genetics**, 26, 364-368. doi: 10.1007/BF00310502

Chen, S., Zhou, Y., Chen, Y., Gu, J. (2018). fastp: an ultra-fast all-in-one FASTQ preprocessor. **Bioinformatics**, 34(17), i884-i890. doi: 10.1093/bioinformatics/bty560

Chessa, R., et al. (2017). Biotechnological exploitation of *Tetrapisispora phaffii* killer toxin: heterologous production in *Komagataella phaffii* (*Pichia pastoris*). **Applied microbiology and biotechnology**, 101(7), 2931-2942. doi: 10.1007/s00253-016-8050-2

Coelho, A. R., Tachi, M., Pagnocca, F. C., Nobrega, G. M. A., Hoffmann, F. L., Harada, K. I., Hirooka, E. Y. (2009). Purification of *Candida guilliermondii* and *Pichia ohmeri* killer toxin as an active agent against *Penicillium expansum*. **Food Additives and Contaminants**, 26(1), 73-81. doi: 10.1080/02652030802227227

Corrêa, M. M., Silva, P. S., Wirth, R., Tabarelli, M., Leal, I. R. (2010). How leaf-cutting ants impact forests: drastic nest effects on light environment and plant assemblages. **Oecologia**, 162, 103-115. doi: 10.1007/s00442-009-1436-4

Crabtree, A. M., Kizer, E. A., Hunter, S. S., Van Leuven, J. T., New, D. D., Fagnan, M. W., Rowley, P. A. (2019). A rapid method for sequencing double-stranded RNAs purified from yeasts and the identification of a potent K1 killer toxin isolated from *Saccharomyces cerevisiae*. **Viruses**, 11(1), 70. doi: 10.3390/v11010070

Crabtree, A. M., Taggart, N. T., Lee, M. D., Boyer, J. M., Rowley, P. A. (2023). The prevalence of killer yeasts and double-stranded RNAs in the budding yeast *Saccharomyces cerevisiae*. **FEMS Yeast Research**, 23, foad046. doi: 10.1093/femsyr/foad046

Craven, S. E., Dix, M. W., Michaels, G. E. (1970). Attine fungus gardens contain yeasts. **Science**, 169(3941), 184–186. doi: 10.1126/science.169.3941.184

Crucitti, D., Chiapello, M., Oliva, D., Forgia, M., Turina, M., Carimi, F., La Bella, F., Pacifico, D. (2021). Identification and molecular characterization of novel mycoviruses in *Saccharomyces* and non-*Saccharomyces* yeasts of oenological interest. **Viruses**, 14(1), 52. doi: 10.3390/v14010052

De Fine Licht, H. H., Boomsma, J. J. (2010). Forage collection, substrate preparation, and diet composition in fungus-growing ants. **Ecological Entomology**, 35(3), 259-269. doi: 10.1111/j.1365-2311.2010.01193.x

Delgado J, Radusky LG, Cianferoni D, Serrano L (2019). FoldX 5.0: Working with RNA, small molecules and a new graphical interface. **Bioinformatics**. 35(20): btz184. doi: 10.1093/bioinformatics/btz184.

Drinnenberg, I. A., Fink, G. R., Bartel, D. P. (2011). Compatibility with killer explains the rise of RNAi-deficient fungi. **Science**, 333(6049), 1592-1592. doi: 10.1126/science.1209575

Drinnenberg, I. A., Weinberg, D. E., Xie, K. T., Mower, J. P., Wolfe, K. H., Fink, G. R., Bartel, D. P. (2009). RNAi in budding yeast. **Science**, 326(5952), 544-550. doi: 10.1126/science.1176945

Farji-brener, A. G., Werenkraut, V. (2015). A meta-analysis of leaf-cutting ant nest effects on soil fertility and plant performance. **Ecological Entomology**, 40(2), 150-158. doi: 10.1111/een.12169

Fisher, P. J., Stradling, D. J., Sutton, B. C., Petrini, L. E. (1996). Microfungi in the fungus gardens of the leaf-cutting ant *Atta cephalotes*: a preliminary study. **Mycological Research**, 100(5), 541–546. doi: 10.1016/S0953-7562(96)80006-2

Frank, A. C., Wolfe, K. H. (2009). Evolutionary capture of viral and plasmid DNA by yeast nuclear chromosomes. **Eukaryotic Cell**, 8(10), 1521-1531. doi: 10.1128/ec.00110-09

Fredericks, L. R., et al. (2021). The species-specific acquisition and diversification of a K1-like family of killer toxins in budding yeasts of the *Saccharomycotina*. **PLoS genetics**, 17(2), e1009341. doi: 10.1371/journal.pgen.1009341

Fuentefria, A. M., Faganello, J., Pazzini, F., Schrank, A., Valente, P., Vainstein, M. (2007). Typing and patterns of cellular morphological alterations in *Cryptococcus neoformans* and *Cryptococcus gattii* isolates exposed to a panel of killer yeasts. **Medical mycology**, 45(6), 503-512. doi: 10.1080/13693780701416580

Fuentefria, A. M., Franskoviaki, I. M., Mercado, L. W., Ramos, J. P., Vainstein, M. H., Valente, P. (2006). Inhibition of clinical and environmental *Cryptococcus neoformans* isolates by two Brasilian killer yeasts. **Journal of basic microbiology**, 46(2), 87-93. doi: 10.1002/jobm.200510018

Fuentefria, A. M., Perez, L. R., Alves d'Azevedo, P., Pazzini, F., Schrank, A., Vainstein, M. H., Valente, P. (2008). Typing of *Staphylococcus epidermidis* clinical strains by a selected panel of Brasilian killer yeasts. **Journal of basic microbiology**, 48(1), 25-30. doi: 10.1002/jobm.200700143

Ganter, P. F., Starmer, W. T. (1992). Killer Factor as a Mechanism of Interference Competition in Yeasts Associated with Cacti: Ecological Archives. **Ecology**, 73(1), 54-67. doi: 10.2307/1938720

Gietz, R. D., Schiestl, R. H., Willems, A. R., Woods, R. A. (1995). Studies on the transformation of intact yeast cells by the LiAc/SS-DNA/PEG procedure. **Yeast**, 11(4), 355-360. doi: 10.1002/yea.320110408

Gimeno, C. J., Ljungdahl, P. O., Styles, C. A., Fink, G. R. (1992). Unipolar cell divisions in the yeast *S. cerevisiae* lead to filamentous growth: regulation by starvation and RAS. **Cell**, 68(6), 1077-1090. doi: 10.1016/0092-8674(92)90079-R

Giometto, A., Nelson, D. R., Murray, A. W. (2021). Antagonism between killer yeast strains as an experimental model for biological nucleation dynamics. **Elife**, 10, e62932. doi: 10.7554/eLife.62932

Giovati, L., et al. (2018). Candidacidal activity of a novel killer toxin from *Wickerhamomyces anomalus* against fluconazole-susceptible and-resistant strains. **Toxins**, 10(2), 68. doi: 10.3390/toxins10020068

Golubev, W. I. (1998). Mycocins (killer toxins). In **The Yeasts** (pp. 55-62). Elsevier. doi: 10.1016/B978-044481312-1/50011-3

Golubev, W. I. (2006). Antagonistic interactions among yeasts. In: Péter, G., Rosa, C. (eds) Biodiversity and Ecophysiology of Yeasts. **The Yeast Handbook**. Springer, Berlin, Heidelberg. doi: 10.1007/3-540-30985-3_10

Golubev, W. I., Pfeiffer, I., Golubeva, E. (2002). Mycocin production in *Trichosporon pullulans* populations colonizing tree exudates in the spring. **FEMS microbiology ecology**, 40(2), 151-157. doi: 10.1111/j.1574-6941.2002.tb00947.x

Goto, K., Iwatuki, Y., Kitano, K., Obata, T., Hara, S. (1990). Cloning and nucleotide sequence of the KHR killer gene of *Saccharomyces cerevisiae*. **Agricultural and biological chemistry**, 54(4), 979-984. doi: 10.1080/00021369.1990.10870081

Goto, K., Fukuda, H., Kichise, K., Kitano, K., Hara, S. (1991). Cloning and nucleotide sequence of the KHS killer gene of *Saccharomyces cerevisiae*. **Agricultural and biological chemistry**, 55(8), 1953-1958. doi: 10.1080/00021369.1991.10870924

Greig, D., Travisano, M. (2008). Density-dependent effects on allelopathic interactions in yeast. **Evolution**, 62(3), 521-527. doi: 10.1111/j.1558-5646.2007.00292.x

Groenewald, M., et al. (2023). A genome-informed higher rank classification of the biotechnologically important fungal subphylum Saccharomycotina. **Studies in Mycology**, 105, 1–22. doi: 10.3114/sim.2023.105.01

Guamán-Burneo, M. C., et al. (2015). Xylitol production by yeasts isolated from rotting wood in the Galápagos Islands, Ecuador, and description of *Cyberlindnera galapagoensis* fa, sp. nov. **Antonie Van Leeuwenhoek**, 108, 919-931. doi: 10.1007/s10482-015-0546-8

Gurevich, A., Saveliev, V., Vyahhi, N., Tesler, G. (2013). QUAST: quality assessment tool for genome assemblies. **Bioinformatics**, 29(8), 1072-1075. doi: 10.1093/bioinformatics/btt086

Harder, C. B. et al. (2023). *Mycena* species can be opportunist-generalist plant root invaders. **Environmental Microbiology**, 25(10), 1875-1893. doi: 10.1111/1462-2920.16398

Hidalgo, P., Flores, M. (1994). Occurrence of the killer character in yeasts associated with Spanish wine production. **Food microbiology**, 11(2), 161-167. doi: 10.1006/fmic.1994.1019

Hodgson, V. J., Button, D., Walker, G. M. (1995). Anti-*Candida* activity of a novel killer toxin from the yeast *Williopsis mrakii*. **Microbiology**, 141(8), 2003-2012. doi:10.1099/13500872-141-8-2003

Houbraken, J. et al. (2020). Classification of *Aspergillus*, *Penicillium*, *Talaromyces* and related genera (Eurotiales): An overview of families, genera, subgenera, sections, series and species. **Studies in mycology**, 95, 5-169. doi: 10.1016/j.simyco.2020.05.002

Ivannikova, Y. V., Naumova, E. S., Naumov, G. I. (2006). Detection of viral dsRNA in the yeast *Saccharomyces bayanus*. **Doklady Biological Sciences**. Vol. 406. New York: Consultants Bureau, c1965-1992. doi: 10.1134/S0012496606010297

Ivannikova, Y. V., Naumova, E. S., Naumov, G. I. (2007). Viral dsRNA in the wine yeast *Saccharomyces bayanus* var. *uvarum*. **Research in microbiology**, 158(8-9), 638-643. doi: 10.1016/j.resmic.2007.07.008

Jones, P., et al. (2014). InterProScan 5: genome-scale protein function classification. **Bioinformatics**, 30(9), 1236-1240. doi: 10.1093/bioinformatics/btu031

Julius D, Brake A, Blair L, Kunisawa R, Thorner J (1984). Isolation of the putative structural gene for the lysine-arginine-cleaving endopeptidase required for processing of yeast prepro-α-factor. **Cell**. 37(3): 1075–1089. doi: 10.1016/0092-8674(84)90442-2.

Jumper, J., et al. (2021). Highly accurate protein structure prediction with AlphaFold. **Nature**, 596(7873), 583-589. doi: 10.1038/s41586-021-03819-2

Jurjevic, Z., Peterson, S. W., Horn, B. W. (2012). *Aspergillus* section *Versicolores*: nine new species and multilocus DNA sequence based phylogeny. **IMA fungus**, 3(1), 59-79. doi:10.5598/imafungus.2012.03.01.07

Károlyi, G., Neufeld, Z., Scheuring, I. (2005). Rock-scissors-paper game in a chaotic flow: The effect of dispersion on the cyclic competition of microorganisms. **Journal of theoretical biology**, 236(1), 12-20. doi: 10.1016/j.jtbi.2005.02.012

Katoh, K., Rozewicki, J., Yamada, K. D. (2019). MAFFT online service: multiple sequence alignment, interactive sequence choice and visualization. **Briefings in Bioinformatics**, 20(4), 1160-1166. doi: 10.1093/bib/bbx108

Kerr, B., Riley, M. A., Feldman, M. W., & Bohannan, B. J. (2002). Local dispersal promotes biodiversity in a real-life game of rock–paper–scissors. **Nature**, 418(6894), 171-174. doi: 10.1038/nature00823

Klassen, R., Meinhardt, F. (2007). Linear protein-primed replicating plasmids in eukaryotic microbes. **Microbial Linear Plasmids**. Berlin, Heidelberg: Springer Berlin Heidelberg, 187-226. doi: 10.1007/7171_2007_095

Klassen, R., Schaffrath, R., Buzzini, P., Ganter, P. F. (2017). Antagonistic interactions and killer yeasts. **Yeasts in natural ecosystems: ecology**, 229-275. doi: 10.1007/978-3-319-61575-2_9

Koltin, Y., Day, P. R. (1976). Suppression of the killer phenotype in *Ustilago maydis*. **Genetics**, 82(4), 629-637. doi: 10.1093/genetics/82.4.629

Krassowski, T., et al. (2018). Evolutionary instability of CUG-Leu in the genetic code of budding yeasts. **Nature communications**, 9(1), 1887. doi: 10.1038/s41467-018-04374-7

Kriventseva, E. V., Kuznetsov, D., Tegenfeldt, F., Manni, M., Dias, R., Simão, F. A., Zdobnov, E. M. (2019). OrthoDB v10: sampling the diversity of animal, plant, fungal, protist, bacterial and viral genomes for evolutionary and functional annotations of orthologs. **Nucleic acids research**, 47(D1), D807-D811. doi: 10.1093/nar/gky1053

Kurtzman, C. P. (2003). Phylogenetic circumscription of *Saccharomyces*, *Kluyveromyces* and other members of the Saccharomycetaceae, and the proposal of the new genera *Lachancea*, *Nakaseomyces*, *Naumovia*, *Vanderwaltozyma* and *Zygotorulaspora*. **FEMS yeast research**, 4(3), 233–245. doi: 10.1016/S1567-1356(03)00175-2.

Kurtzman C. P., Robnett, C. J. (1998) Identification and phylogeny of ascomycetous yeasts from analysis of nuclear large subunit (26S) ribosomal DNA partial sequences. **Antonie Van Leeuwenhoek,** 73(4):331–371. doi: 10.1023/a:1001761008817.

Kurtzman, C. P., Robnett, C. J. (2003). Phylogenetic relationships among yeasts of the '*Saccharomyces* complex' determined from multigene sequence analyses. **FEMS yeast research**, 3(4), 417-432. doi: 10.1016/S1567-1356(03)00012-6

Laetsch, D. R., Blaxter, M. L. (2017). BlobTools: Interrogation of genome assemblies. **F1000Research**, 6(1287), 1287. doi: 10.12688/f1000research.12232.1

Leal, I. R., Oliveira, P. S. (1998). Interactions between Fungus-Growing Ants (Attini), Fruits and Seeds in Cerrado Vegetation in Southeast Brasil. **Biotropica**, 30(2), 170-178. doi: 10.1111/j.1744-7429.1998.tb00052.x

Lee, M. D., Creagh, J. W., Fredericks, L. R., Crabtree, A. M., Patel, J. S., Rowley, P. A. (2022). The Characterization of a Novel Virus Discovered in the Yeast *Pichia membranifaciens*. **Viruses**, 14(3), 594. doi: 10.3390/v14030594

Li, H. (2018). Minimap2: pairwise alignment for nucleotide sequences. **Bioinformatics**, 34(18), 3094-3100. doi: 10.1093/bioinformatics/bty191

Li, H., et al. (2009). The sequence alignment/map format and SAMtools. **Bioinformatics**, 25(16), 2078-2079. doi: 10.1093/bioinformatics/btp352

Libberton, B., Horsburgh, M. J., Brockhurst, M. A. (2015). The effects of spatial structure, frequency dependence and resistance evolution on the dynamics of toxin-mediated microbial invasions. **Evolutionary applications**, 8(7), 738-750. doi: 10.1111/eva.12284

Liu, H., Fu, Y., Jiang, D., Li, G., Xie, J., Cheng, J., Peng, Y., Ghabrial, S. A. Yi, X. (2010). Widespread horizontal gene transfer from double-stranded RNA viruses to eukaryotic nuclear genomes. **Journal of virology**, 84(22), 11876-11887. doi: 10.1128/jvi.00955-10

Liu, F., et al. (2024). *Saccharomycetaceae*: delineation of fungal genera based on phylogenomic analyses, genomic relatedness indices and genomics-based synapomorphies. **Persoonia**, 52(1), 1-21. doi: 10.3767/persoonia.2024.52.01.

Lomsadze, A., Ter-Hovhannisyan, V., Chernoff, Y. O., Borodovsky, M. (2005). Gene identification in novel eukaryotic genomes by self-training algorithm. **Nucleic acids research**, 33(20), 6494-6506. doi: 10.1093/nar/gki937

Lu, S., Faris, J. D. (2019). *Fusarium graminearum* KP4-like proteins possess root growth-inhibiting activity against wheat and potentially contribute to fungal virulence in seedling rot. **Fungal genetics and biology**, 123, 1-13. doi: 10.1016/j.fgb.2018.11.002

Madbouly, A. K., Elyousr, K. A. A., Ismail, I. M. (2020). Biocontrol of *Monilinia fructigena*, causal agent of brown rot of apple fruit, by using endophytic yeasts. **Biological control**, 144, 104239. doi: 10.1016/j.biocontrol.2020.104239

Magliani, W., Conti, S., Gerloni, M., Bertolotti, D., Polonelli, L. (1997). Yeast killer systems. **Clinical microbiology reviews**, 10(3), 369-400. doi: 10.1128/cmr.10.3.369

Makower, M., Bevan, E. A. (1963). The inheritance of a killer character in yeast (*Saccharomyces cerevisiae*). **Genetics today. Proceedings of the XI International Congress of Genetics**, v. 1, 202.

Maksimova, I. A., Glushakova, A. M., Kachalkin, A. V., Chernov, I. Y., Panteleeva, S. N., Reznikova, Z. I. (2016). Yeast communities of Formica aquilonia colonies. **Microbiology**, 85, 124-129. doi: 10.1134/S0026261716010045

Marquina, D., Santos, A., Peinado, J. (2002). Biology of killer yeasts. **International Microbiology**, 5, 65-71. doi: 10.1007/s10123-002-0066-z

McBride, R., Greig, D., Travisano, M. (2008). Fungal viral mutualism moderated by ploidy. **Evolution**, 62(9), 2372-2380. doi: 10.1111/j.1558-5646.2008.00443.x

Meyer, W., Mitchell, T.G., Freedman, E.Z., Vilgalys, R. (1993) Hybridization probes for conventional DNA fingerprinting used as single primers in the polymerase chain reaction to distinguish strains of *Cryptococcus neoformans*. **Journal of Clinical Microbiology**, 31(9):2274–2280. doi: 10.1128/jcm.31.9.2274-2280.1993.

Meyer, S. T., Leal, I. R., Tabarelli, M., Wirth, R. (2011). Ecosystem engineering by leaf-cutting ants: nests of *Atta cephalotes* drastically alter forest structure and microclimate. **Ecological entomology**, 36(1), 14-24. doi: 10.1111/j.1365-2311.2010.01241.x

Middelbeek, E. J., Hermans, J. M., Stumm, C., Muytjens, H. L. (1980). High incidence of sensitivity to yeast killer toxins among *Candida* and *Torulopsis* isolates of human origin. **Antimicrobial Agents and Chemotherapy**, 17(3), 350-354. doi: 10.1128/aac.17.3.350

Möller, A. (1893). **Die Pilzgärten einiger südamerikanischer Ameisen** (No. 6). G. Fischer.

Myers, J. M., et al. (2020). Survey of early-diverging lineages of fungi reveals abundant and diverse mycoviruses. **mBio** 11: e02027-20. doi: 10.1128/mbio.02027-20

Naumov, G. I., Ivannikova, Y. V., Chernov, I. Y., Naumova, E. S. (2009). Natural polymorphism of the plasmid double-stranded RNA of the *Saccharomyces* yeasts. **Microbiology**, 78, 208-213. doi: 10.1134/S0026261709020118

Nguyen, L. T., Schmidt, H. A., Von Haeseler, A., Minh, B. Q. (2015). IQ-TREE: a fast and effective stochastic algorithm for estimating maximum-likelihood phylogenies. **Molecular Biology and Evolution**, 32(1), 268-274. doi: 10.1093/molbev/msu300

Nguyen, N. H., Suh, S. O., Blackwell, M. (2007). Five novel *Candida* species in insect-associated yeast clades isolated from Neuroptera and other insects. **Mycologia**, 99(6), 842–858. doi: 10.1080/15572536.2007.11832516

Nomoto, H., Kitano, K., Shimazaki, T., Kodama, K., Hara, S. (1984). Distribution of killer yeasts in the genus *Hansenula*. **Agricultural and biological chemistry**, 48(3), 807-809. doi: 10.1271/bbb1961.48.807

Nygaard, S., et al. (2016). Reciprocal genomic evolution in the ant–fungus agricultural symbiosis. **Nature Communications**, 7(1), 12233. doi: 10.1038/ncomms12233

Okada, R., Kiyota, E., Moriyama, H., Fukuhara, T., Natsuaki, T. (2015). A simple and rapid method to purify viral dsRNA from plant and fungal tissue. **Journal of General Plant Pathology**, 81, 103-107. doi: 10.1007/s10327-014-0575-6

Pagnocca, F. C., Carreiro, S. C., Bueno, O. C., Hebling, M. J., Da Silva, O. A. (1996). Microbiological changes in the nests of leaf-cutting ants fed on sesame leaves. **Journal of Applied Entomology**, 120(1-5), 317–320. doi: 10.1111/j.1439-0418.1996.tb01612.x

Pagnocca, F. C., Rodrigues, A., Nagamoto, N. S., Bacci, M. (2008). Yeasts and filamentous fungi carried by the gynes of leaf-cutting ants. **Antonie van Leeuwenhoek**, 94(4), 517–526. doi: 10.1007/s10482-008-9268-5

Perez, M. F., Contreras, L., Garnica, N. M., Fernández-Zenoff, M. V., Farías, M. E., Sepulveda, M., Ramallo, J., Dib, J. R. (2016). Native killer yeasts as biocontrol agents of postharvest fungal diseases in lemons. **PloS One**, 11(10), e0165590. doi: 10.1371/journal.pone.0165590

Peterson, S. W., Ito, Y., Horn, B. W., Goto, T. (2001). *Aspergillus bombycis*, a new aflatoxigenic species and genetic variation in its sibling species, *A. nomius*. **Mycologia**, 93(4), 689-703. doi: 10.1080/00275514.2001.12063200

Pfeiffer, I., Golubev, W. I., Farkas, Z., Kucsera, J., Golubev, N. (2004). Mycocin production in *Cryptococcus aquaticus*. **Antonie Van Leeuwenhoek**, 86, 369-375. doi: 10.1007/s10482-004-0888-0

Philliskirk, G., Young, T. W. (1975). The occurrence of killer character in yeasts of various genera. **Antonie van Leeuwenhoek**, 41, 147-151. doi: 10.1007/BF02565046

Pieczynska, M. D., de Visser, J. A. G., Korona, R. (2013). Incidence of symbiotic dsRNA 'killer' viruses in wild and domesticated yeast. **FEMS Yeast Research**, 13(8), 856–859. doi: 10.1111/1567-1364.12086

Pieczynska, M. D., Wloch-Salamon, D., Korona, R., de Visser, J. A. G. (2016). Rapid multiple-level coevolution in experimental populations of yeast killer and nonkiller strains. **Evolution**, 70(6), 1342-1353. doi: 10.1111/evo.12945

Pintar, J., Starmer, W. T. (2003). The costs and benefits of killer toxin production by the yeast Pichia kluyveri. **Antonie van Leeuwenhoek**, 83, 89-97. doi: 10.1023/A:0000000089097

Posit team (2023). RStudio: Integrated Development Environment for R. Posit Software, PBC, Boston, MA. URL http://www.posit.co/.

R Core Team. (2023). R: A Language and Environment for Statistical Computing.; **R Foundation for Statistical Computing: Vienna, Austria**; Available online: https://www.R-project.org/

Ramachandran GN, Ramakrishnan C, Sasisekharan V (1963). Stereochemistry of polypeptide chain configurations. **J Mol Biol**. 7(1): 95–99. doi: 10.1016/s0022-2836(63)80023-6.

Rambaut, A., 2016. **Figtree v. 1.4.3**. http://tree.bio.ed.ac.uk/software/figtree/2016.

Ramírez, M., Velázquez, R., Maqueda, M., López-Piñeiro, A., Ribas, J. C. (2015). A new wine *Torulaspora delbrueckii* killer strain with broad antifungal activity and its toxin-encoding double-stranded RNA virus. **Frontiers in microbiology**, 6, 983. doi: 10.3389/fmicb.2015.00983

Robledo-Leal, E., Elisondo-Zatuche, M., Treviño-Rangel, R. J., González, G. M., Hernández-Luna, C. (2016). Isolation of killer yeasts from ants of the genus *Atta* and their effect on the red tomato's fungal pathogen *Geotrichum candidum*. **Mexican Journal of Phytopathology**, 34, 258–269. doi: 10.18781/r.mex.fit.1605-3

Rodrigues, A., Bacci Jr, M., Mueller, U. G., Ortiz, A., Pagnocca, F. C. (2008). Microfungal "weeds" in the leafcutter ant symbiosis. **Microbial Ecology**, 56, 604-614. doi: 10.1007/s00248-008-9380-0

Rodrigues, A., Cable, R. N., Mueller, U. G., Bacci, M., Pagnocca, F. C. (2009). Antagonistic interactions between garden yeasts and microfungal garden pathogens of leaf-cutting ants. **Antonie Van Leeuwenhoek**, 96, 331-342. doi: 10.1007/s10482-009-9350-7

Rodríguez-Cousiño, N., Gómez, P., Esteban, R. (2017). Variation and distribution of LA helper totiviruses in *Saccharomyces* sensu stricto yeasts producing different killer toxins. Toxins, 9(10), 313. doi: doi.org/10.3390/toxins9100313

Rodríguez-Cousiño, N., Maqueda, M., Ambrona, J., Zamora, E., Esteban, R., Ramírez, M. (2011). A new wine *Saccharomyces cerevisiae* killer toxin (Klus), encoded by a double-stranded RNA virus, with broad antifungal activity is evolutionarily related to a chromosomal

host gene. **Applied and environmental microbiology**, 77(5), 1822-1832. doi: 10.1128/AEM.02501-10

Rodriguez Coy, L., Plummer, K. M., Khalifa, M. E., MacDiarmid, R. M. (2022). Mycovirus-encoded suppressors of RNA silencing: Possible allies or enemies in the use of RNAi to control fungal disease in crops. **Frontiers in Fungal Biology**, 3, 965781. doi: 10.3389/ffunb.2022.965781

Ronque, M. U., Feitosa, R. M., Oliveira, P. S. (2019). Natural history and ecology of fungus-farming ants: a field study in Atlantic rainforest. **Insectes Sociaux**, 66(3), 375-387. doi: 10.1007/s00040-019-00695-y

Rowley, P. A. (2017). The frenemies within: viruses, retrotransposons and plasmids that naturally infect *Saccharomyces* yeasts. **Yeast**, 34(7), 279-292. doi: 10.1002/yea.3234

Rupert, C. B., Rusche, L. N. (2022). The Pathogenic Yeast *Candida parapsilosis* Forms Pseudohyphae through Different Signaling Pathways Depending on the Available Carbon Source. **Msphere**, 7(3), e00029-22. doi: 10.1128/msphere.00029-22

Satwika, D., Klassen, R., Meinhardt, F. (2012). Repeated capture of a cytoplasmic linear plasmid by the host nucleus in *Debaryomyces hansenii*. **Yeast**, 29(3-4), 145-154. doi: 10.1002/yea.2893

Schaffrath, R., Meinhardt, F., Klassen, R. (2018). Yeast killer toxins: Fundamentals and applications. **Physiology and Genetics: Selected Basic and Applied Aspects**, 87-118. doi: 10.1007/978-3-319-71740-1_3

Schmitt, M. J., Neuhausen, F. (1994). Killer toxin-secreting double-stranded RNA mycoviruses in the yeasts *Hanseniaspora uvarum* and *Zygosaccharomyces bailii*. **Journal of virology**, 68(3), 1765-1772. doi: 10.1128/jvi.68.3.1765-1772.1994

Schneider, C. A., Rasband, W. S., Eliceiri, K. W. (2012). NIH Image to ImageJ: 25 years of image analysis. **Nature methods**, 9(7), 671-675. doi: 10.1038/nmeth.2089

Schultz, T. R., Brady, S. G. (2008). Major evolutionary transitions in ant agriculture. **Proceedings of the National Academy of Sciences**, 105(14), 5435–5440. doi: 10.1073/pnas.0711024105

Schultz, T. R., Sosa-Calvo, J., Brady, S. G., Lopes, C. T., Mueller, U. G., Bacci Jr, M., Vasconcelos, H. L. (2015). The most relictual fungus-farming ant species cultivates the most recently evolved and highly domesticated fungal symbiont species. **The American Naturalist**, 185(5), 693–703. doi: 10.1086/680501

Segers, G. C., van Wezel, R., Zhang, X., Hong, Y., Nuss, D. L. (2006). Hypovirus papain-like protease p29 suppresses RNA silencing in the natural fungal host and in a heterologous plant system. **Eukaryotic Cell**, 5(6), 896-904. doi: 10.1128/EC.00373-05

Segers, G. C., Zhang, X., Deng, F., Sun, Q., Nuss, D. L. (2007). Evidence that RNA silencing functions as an antiviral defense mechanism in fungi. **Proceedings of the National Academy of Sciences**, 104(31), 12902-12906. doi: 10.1073/pnas.070250010

Seppey, M., Manni, M., Zdobnov, E.M. (2019). BUSCO: Assessing Genome Assembly and Annotation Completeness. In: Kollmar, M. (eds) Gene Prediction. **Methods in Molecular Biology**, vol 1962. Humana, New York, NY. doi: 10.1007/978-1-4939-9173-0_14

Silva, A., Bacci Jr, M., de Siqueira, C. G., Bueno, O. C., Pagnocca, F. C., Hebling, M. J. A. (2003). Survival of *Atta sexdens* workers on different food sources. **Journal of Insect Physiology**, 49(4), 307-313. doi: 10.1016/S0022-1910(03)00004-0

Silva, A., Bacci Jr, M., Pagnocca, F. C., Bueno, O. C., Hebling, M. J. A. (2006). Starch metabolism in *Leucoagaricus gongylophorus*, the symbiotic fungus of leaf-cutting ants. **Microbiological research**, 161(4), 299-303. doi: 10.1016/j.micres.2005.11.001

Somers, J. M., Bevan, E. A. (1969). The inheritance of the killer character in yeast. **Genetics Research**, 13(1), 71-83. doi: 10.1017/S0016672300002743

Spoel D. V. D., Lindahl E, Hess B, Groenhof G, Mark AE, Berendsen HJC (2005). GROMACS: Fast, flexible, and free. **J Comput Chem**. 26(16): 1701–1718. doi: 10.1002/jcc.20291.

Stanke, M., Morgenstern, B. (2005). AUGUSTUS: a web server for gene prediction in eukaryotes that allows user-defined constraints. **Nucleic acids research**, 33(suppl_2), W465-W467. doi: 10.1093/nar/gki458

Starmer, W. T., Ganter, P. F., Aberdeen, V., Lachance, M. A., Phaff, H. J. (1987). The ecological role of killer yeasts in natural communities of yeasts. **Canadian journal of microbiology**, 33(9), 783-796. doi: 10.1139/m87-134

Sternberg, L. D. S., Pinzon, M. C., Moreira, M. Z., Moutinho, P., Rojas, E. I., Herre, E. A. (2007). Plants use macronutrients accumulated in leaf-cutting ant nests. **Proceedings of the Royal Society B: Biological Sciences**, 274(1608), 315-321. doi: 10.1098/rspb.2006.3746

Stopiglia, C. D. O., Heidrich, D., Sorrentino, J. M., Vieira, F. J., Landell, M. F., Valente, P., Scroferneker, M. L. (2014). Susceptibility of species within the *Sporothrix schenckii* complex to a panel of killer yeasts. **Journal of Basic Microbiology**, 54(6), 578-584. doi: 10.1002/jobm.201200516

Studer G, Rempfer C, Waterhouse AM, Gumienny R, Haas J, Schwede T (2019). QMEANDisCo – Distance Constraints Applied on Model Quality Estimation. **Bioinformatics**. 36(6): 1765–1771. doi: 10.1093/bioinformatics/btz828.

Stumm, C., Hermans, J. M. H., Middelbeek, E. J., Croes, A. F., De Vries, G. J. M. L. (1977). Killer-sensitive relationships in yeasts from natural habitats. **Antonie van Leeuwenhoek**, 43, 125-128. doi: 10.1007/BF00395667

Suh, S. O., Blackwell, M. (2005). Four new yeasts in the *Candida mesenterica* clade associated with basidiocarp-feeding beetles. **Mycologia**, 97(1), 167-177. doi: 10.1080/15572536.2006.11832850

Suh, S. O., McHugh, J. V., Pollock, D. D., Backwell, M. (2005). The beetle gut: a hyperdiverse source of novel yeasts. **Mycological Research**, 109(3), 261–265. doi: 10.1017/S0953756205002388

Summerell, B. A., Laurence, M. H., Liew, E. C., Leslie, J. F. (2010). Biogeography and phylogeography of *Fusarium*: a review. **Fungal Diversity**, 44(1), 3-13. doi: 10.1007/s13225-010-0060-2

Suzuki, C., Nikkuni, S. (1994). The primary and subunit structure of a novel type killer toxin produced by a halotolerant yeast, *Pichia farinosa*. **Journal of Biological Chemistry**, 269(4), 3041-3046. doi: 10.1016/S0021-9258(17)42044-8

Taylor, D. J., Ballinger, M. J., Bowman, S. M., Bruenn, J. A. (2013). Virus-host co-evolution under a modified nuclear genetic code. **PeerJ**, 1, e50. doi: 10.7717/peerj.50

Taylor, D. J., Bruenn, J. (2009). The evolution of novel fungal genes from non-retroviral RNA viruses. **BMC biology**, 7, 1-11. doi: 10.1186/1741-7007-7-88

Thoen, E., et al. (2020). In vitro evidence of root colonization suggests ecological versatility in the genus *Mycena*. **New Phytologist**, 227(2), 601-612. doi: 10.1111/nph.16545

Travers-Cook, T. J., Jokela, J., Buser, C. C. (2023). The evolutionary ecology of fungal killer phenotypes. **Proceedings of the Royal Society B**, 290, 20231108. doi: 10.1098/rspb.2023.1108

Trindade, R. C., Resende, M. A., Silva, C. M., Rosa, C. A. (2002). Yeasts associated with fresh and frozen pulps of Brasilian tropical fruits. **Systematic and Applied Microbiology**, 25(2), 294-300. doi: 10.1078/0723-2020-00089

Vadasz, A. S., Vadasz, P., Gupthar, A. S., Abashar, M. E. (2003). Theoretical and experimental evidence of extinction and coexistence of killer and sensitive strains of yeast grown as a mixed culture in water. **International journal of food microbiology**, 84(2), 157-174. doi: 10.1016/S0168-1605(02)00417-8

Vaughan-Martini, A. (1995). *Saccharomyces barnetti* and *Saccharomyces spencerorum*: two new species of *Saccharomyces* sensu lato (van der Walt). **Antonie van Leeuwenhoek**, 68, 111-118. doi: 10.1007/BF00873098

Vijayraghavan, S., Kozmin, S. G., Strope, P. K., Skelly, D. A., Magwene, P. M., Dietrich, F. S., McCusker, J. H. (2023). RNA viruses, M satellites, chromosomal killer genes, and killer/nonkiller phenotypes in the 100-genomes *S. cerevisiae* strains. **G3: Genes, Genomes, Genetics**, 13(10), jkad167. doi: 10.1093/g3journal/jkad167

Villan Larios, et al. (2023). Exploring the Mycovirus Universe: Identification, Diversity, and Biotechnological Applications. **Journal of Fungi**, 9(3), 361. doi: 10.3390/jof9030361

Walker, G. M., Mcleod, A. H., Hodgson, V. J. (1995). Interactions between killer yeasts and pathogenic fungi. **FEMS microbiology letters**, 127(3), 213-222. doi: 10.1111/j.1574-6968.1995.tb07476.x

Warnes, G., Bolker, B., Bonebakker, L., Gentleman, R., Huber, W., Liaw, A., Lumley, T., Maechler, M., Magnusson, A., Moeller, S., Schwartz, M., Venables, B., Galili, T. (2024). *gplots*: Various R Programming Tools for Plotting Data. **R package version 3.2.0**. doi: 10.32614/CRAN.package.gplots

Weber, N. A. (1972). The fungus-culturing behavior of ants. **American Zoologist**, 12(3), 577–587. doi: 10.1093/icb/12.3.577

Wickham H (2016). ggplot2: Elegant Graphics for Data Analysis. Springer-Verlag New York. ISBN 978-3-319-24277-4, https://ggplot2.tidyverse.org.

Wloch-Salamon, D. M., Gerla, D., Hoekstra, R. F., de Visser, J. A. G. (2008). Effect of dispersal and nutrient availability on the competitive ability of toxin-producing yeast. **Proceedings of the Royal Society B: Biological Sciences**, 275(1634), 535-541. doi: 10.1098/rspb.2007.1461

Wójcik, M., Kordowska-Wiater, M. (2015). The occurrence of killer activity in yeasts isolated from natural habitats. **Acta Biochimica Polonica**, 62(4). doi: 10.18388/abp.2015_1141

Woods, D. R., Bevan, E. A. (1968). Studies on the nature of the killer factor produced by *Saccharomyces cerevisiae*. **Microbiology**, 51(1), 115–126. doi: 10.1099/00221287-51-1-115

Worsham, P. L., Bolen, P. L. (1990). Killer toxin production in *Pichia acaciae* is associated with linear DNA plasmids. **Current genetics**, 18, 77-80. doi: 10.1007/BF00321119

Zorg, J., Kilian, S., Radler, F. (1988). Killer toxin producing strains of the yeasts *Hanseniaspora uvarum* and *Pichia kluyveri*. **Archives of microbiology**, 149, 261-267. doi: 10.1007/BF00422015

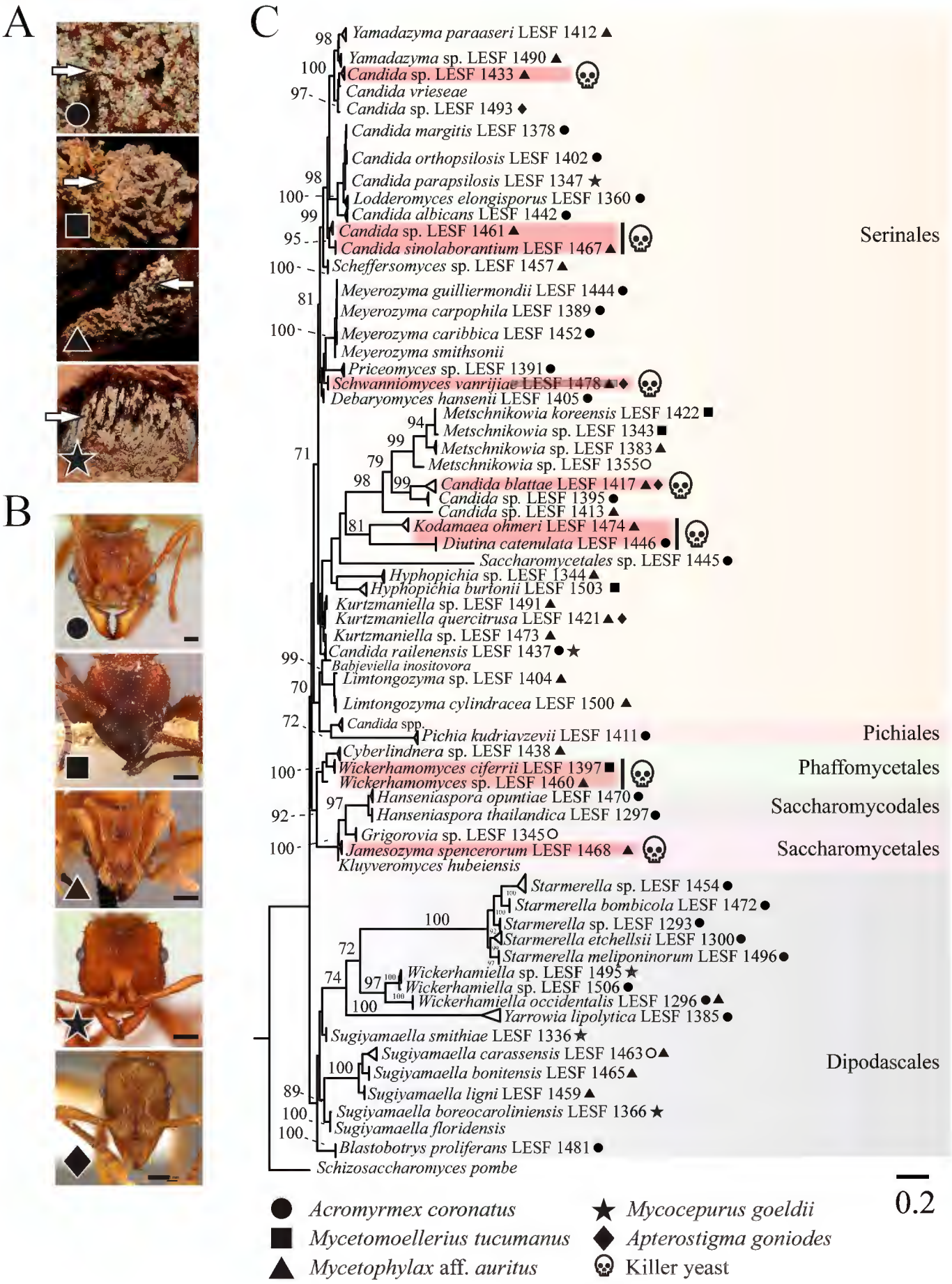
A
B
C
Yamadazyma paraaseri LESF 1412
Yamadazyma sp. LESF 1490
Candida sp. LESF 1433
Candida vrieseae
Candida sp. LESF 1493
Candida margitis LESF 1378
Candida orthopsilosis LESF 1402
Candida parapsilosis LESF 1347
Lodderomyces elongisporus LESF 1360
Candida albicans LESF 1442
Candida sp. LESF 1461
Candida sinolaborantium LESF 1467
Scheffersomyces sp. LESF 1457
Meyerozyma guilliermondii LESF 1444
Meyerozyma carpophila LESF 1389
Meyerozyma caribbica LESF 1452
Meyerozyma smithsonii
Priceomyces sp. LESF 1391
Schwanniomyces vanrijiae LESF 1478
Debaryomyces hansenii LESF 1405
Metschnikowia koreensis LESF 1422
Metschnikowia sp. LESF 1343
Metschnikowia sp. LESF 1383
Metschnikowia sp. LESF 1355
Candida blattae LESF 1417
Candida sp. LESF 1395
Candida sp. LESF 1413
Kodamaea ohmeri LESF 1474
Diutina catenulata LESF 1446
Saccharomycetales sp. LESF 1445
Hyphopichia sp. LESF 1344
Hyphopichia burtonii LESF 1503
Kurtzmaniella sp. LESF 1491
Kurtzmaniella quercitrusa LESF 1421
Kurtzmaniella sp. LESF 1473
Candida railenensis LESF 1437
Babjeviella inositovora
Limtongozyma sp. LESF 1404
Limtongozyma cylindracea LESF 1500
Candida spp.
Pichia kudriavzevii LESF 1411
Cyberlindnera sp. LESF 1438
Wickerhamomyces ciferrii LESF 1397
Wickerhamomyces sp. LESF 1460
Hanseniaspora opuntiae LESF 1470
Hanseniaspora thailandica LESF 1297
Grigorovia sp. LESF 1345
Jamesozyma spencerorum LESF 1468
Kluyveromyces hubeiensis
Starmerella sp. LESF 1454
Starmerella bombicola LESF 1472
Starmerella sp. LESF 1293
Starmerella etchellsii LESF 1300
Starmerella meliponinorum LESF 1496
Wickerhamiella sp. LESF 1495
Wickerhamiella sp. LESF 1506
Wickerhamiella occidentalis LESF 1296
Yarrowia lipolytica LESF 1385
Sugiyamaella smithiae LESF 1336
Sugiyamaella carassensis LESF 1463
Sugiyamaella bonitensis LESF 1465
Sugiyamaella ligni LESF 1459
Sugiyamaella boreocaroliniensis LESF 1366
Sugiyamaella floridensis
Blastobotrys proliferans LESF 1481
Schizosaccharomyces pombe
Serinales
Pichiales
Phaffomycetales
Saccharomycodales
Saccharomycetales
Dipodascales
0.2
Acromyrmex coronatus
Mycetomoellerius tucumanus
Mycetophylax aff. auritus
Mycocepurus goeldii
Apterostigma goniodes
Killer yeast

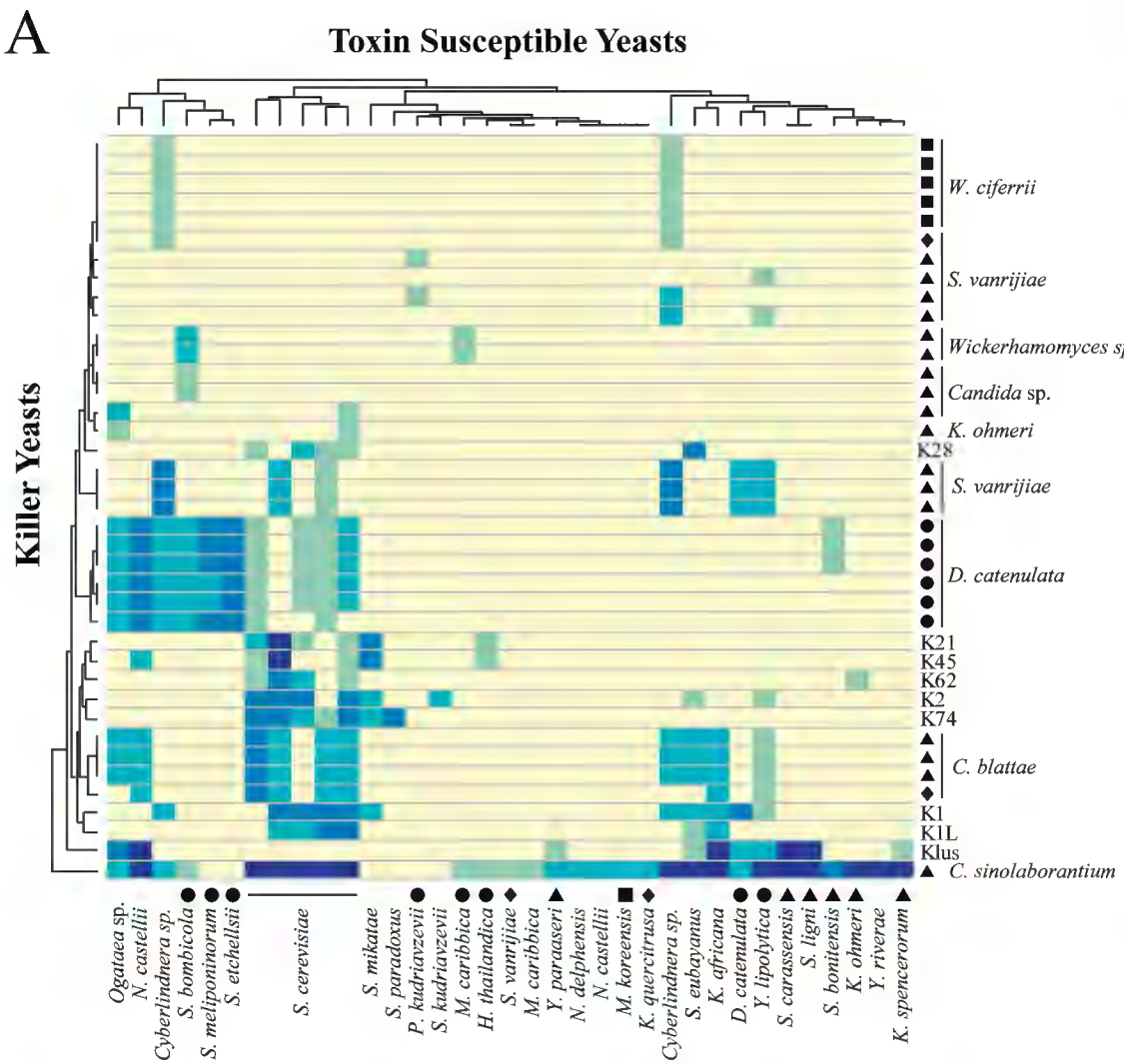

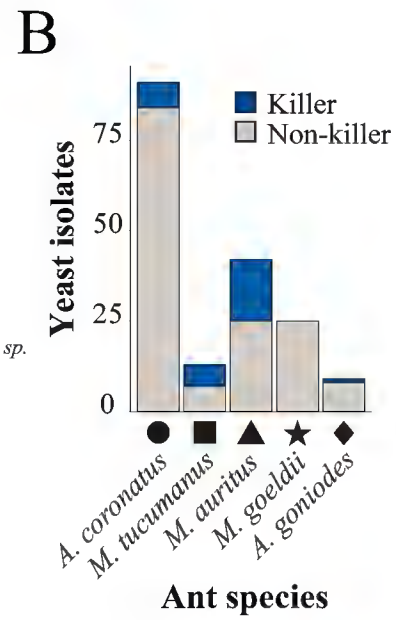

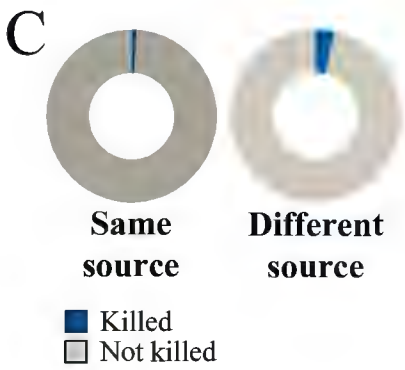

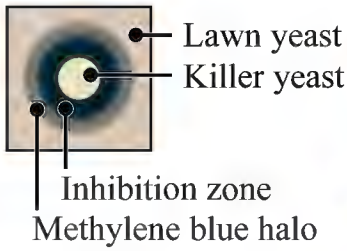

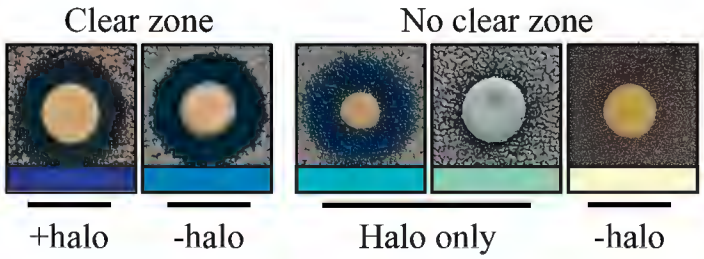

- ● *Acromyrmex coronatus*
- ■ *Mycetomoellerius tucumanus*
- ▲ *Mycetophylax* aff. *auritus*
- ★ *Mycocepurus goeldii*
- ◆ *Apterostigma goniodes*

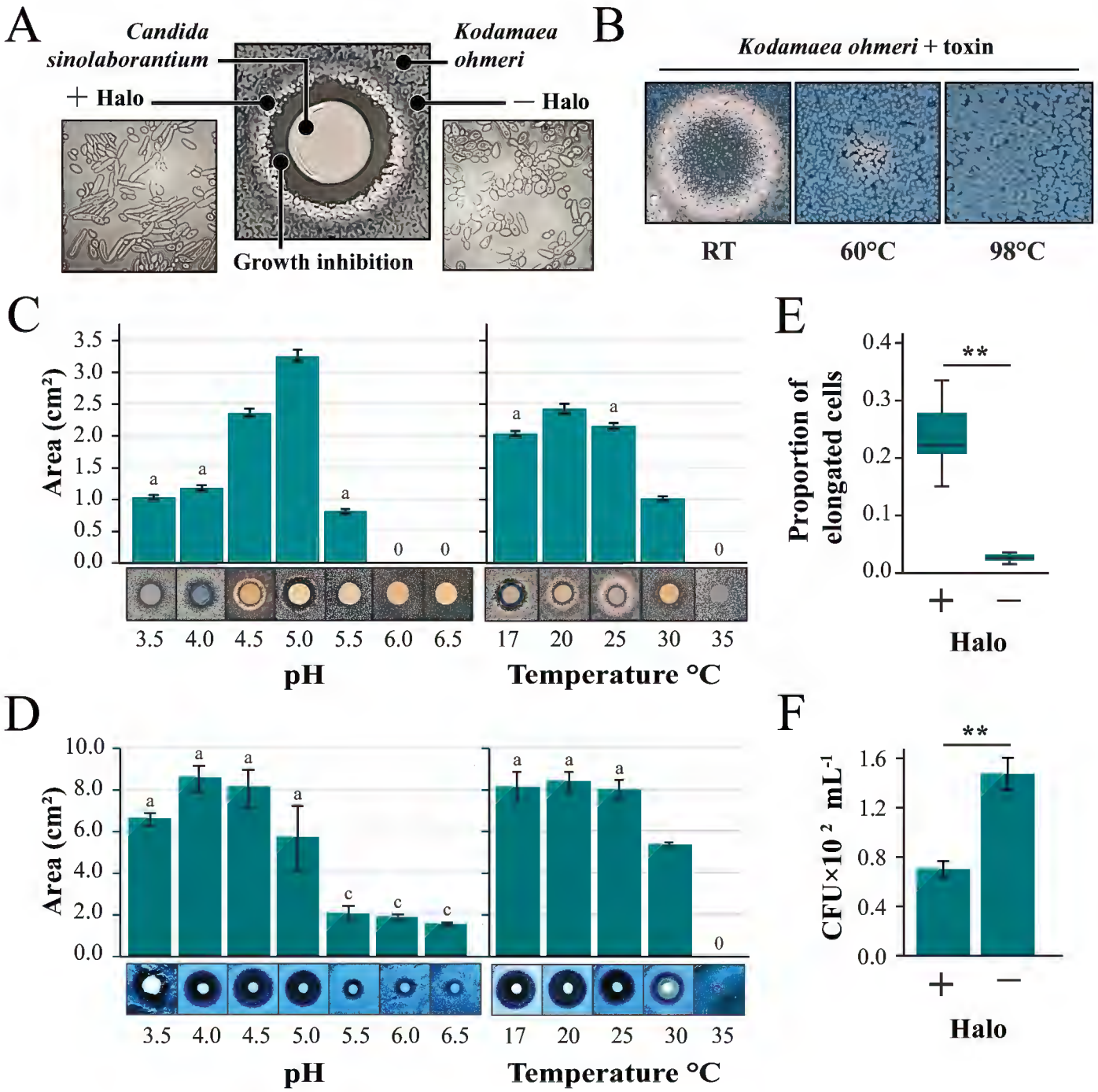
A
Candida sinolaborantium
Kodamaea ohmeri
+ Halo
— Halo
Growth inhibition
B
Kodamaea ohmeri + toxin
RT
60°C
98°C
C
Area (cm²)
3.5
3.0
2.5
2.0
1.5
1.0
0.5
0.0
a
a
a
0
0
a
a
0
3.5 4.0 4.5 5.0 5.5 6.0 6.5
pH
17 20 25 30 35
Temperature °C
E
Proportion of elongated cells
0.4
0.3
0.2
0.1
0.0
**
+
—
Halo
D
Area (cm²)
10.0
8.0
6.0
4.0
2.0
0.0
a
a
a
a
c
c
c
a
a
a
0
3.5 4.0 4.5 5.0 5.5 6.0 6.5
pH
17 20 25 30 35
Temperature °C
F
CFU×10 ² mL-1
1.6
1.2
0.8
0.4
0.0
**
+
—
Halo

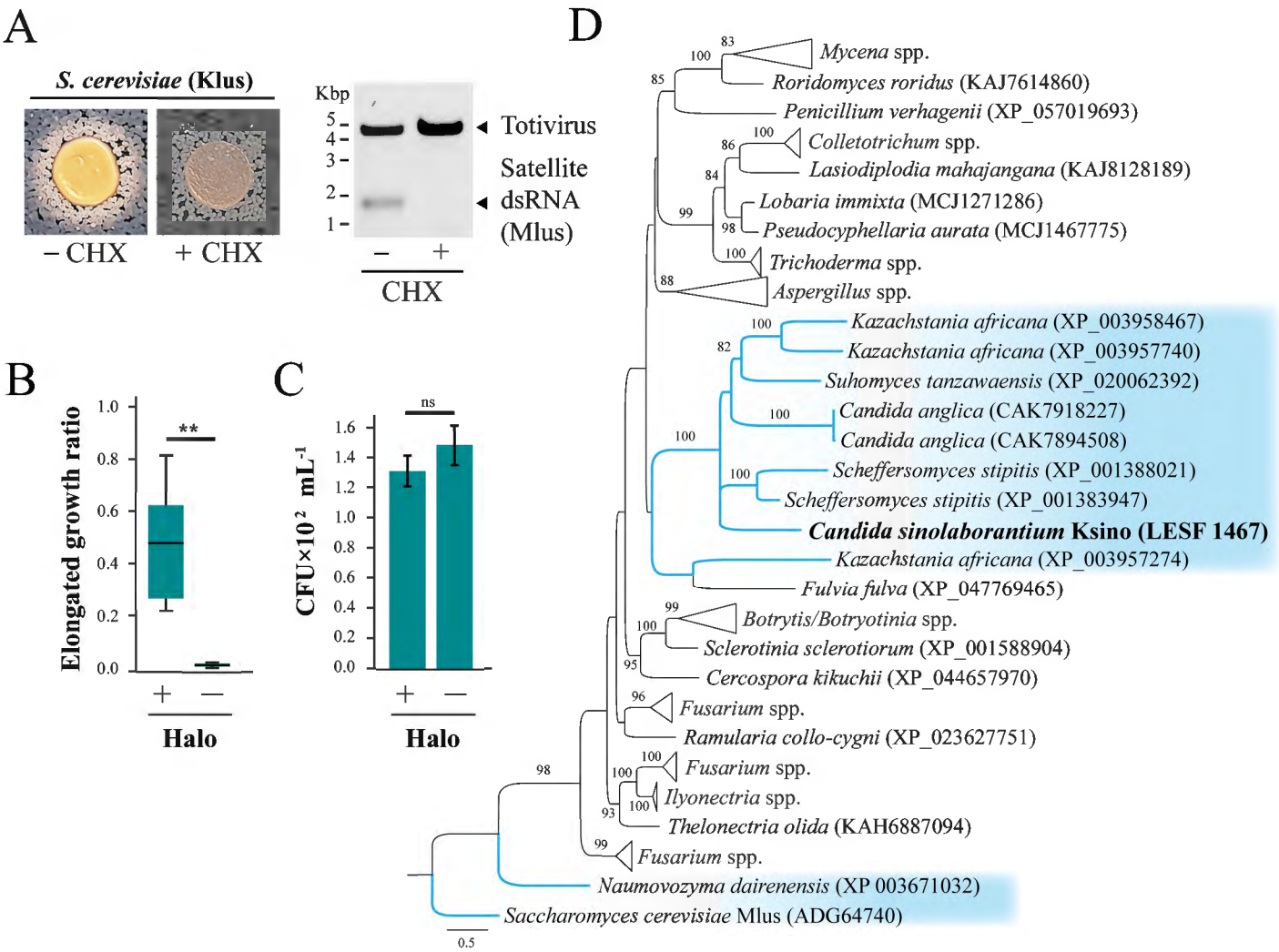
A
S. cerevisiae (Klus)
− CHX
+ CHX
Kbp
5
4
3
2
1
Totivirus
Satellite
dsRNA
(Mlus)
−
+
CHX
B
Elongated growth ratio
1.0
0.8
0.6
0.4
0.2
0.0
**
+
−
Halo
C
CFU×10² mL⁻¹
1.6
1.4
1.2
1.0
0.8
0.6
0.4
0.2
0.0
ns
+
−
Halo
D
Mycena spp.
Roridomyces roridus (KAJ7614860)
Penicillium verhagenii (XP_057019693)
Colletotrichum spp.
Lasiodiplodia mahajangana (KAJ8128189)
Lobaria immixta (MCJ1271286)
Pseudocyphellaria aurata (MCJ1467775)
Trichoderma spp.
Aspergillus spp.
Kazachstania africana (XP_003958467)
Kazachstania africana (XP_003957740)
Suhomyces tanzawaensis (XP_020062392)
Candida anglica (CAK7918227)
Candida anglica (CAK7894508)
Scheffersomyces stipitis (XP_001388021)
Scheffersomyces stipitis (XP_001383947)
Candida sinolaborantium Ksino (LESF 1467)
Kazachstania africana (XP_003957274)
Fulvia fulva (XP_047769465)
Botrytis/Botryotinia spp.
Sclerotinia sclerotiorum (XP_001588904)
Cercospora kikuchii (XP_044657970)
Fusarium spp.
Ramularia collo-cygni (XP_023627751)
Fusarium spp.
Ilyonectria spp.
Thelonectria olida (KAH6887094)
Fusarium spp.
Naumovozyma dairenensis (XP 003671032)
Saccharomyces cerevisiae Mlus (ADG64740)
0.5

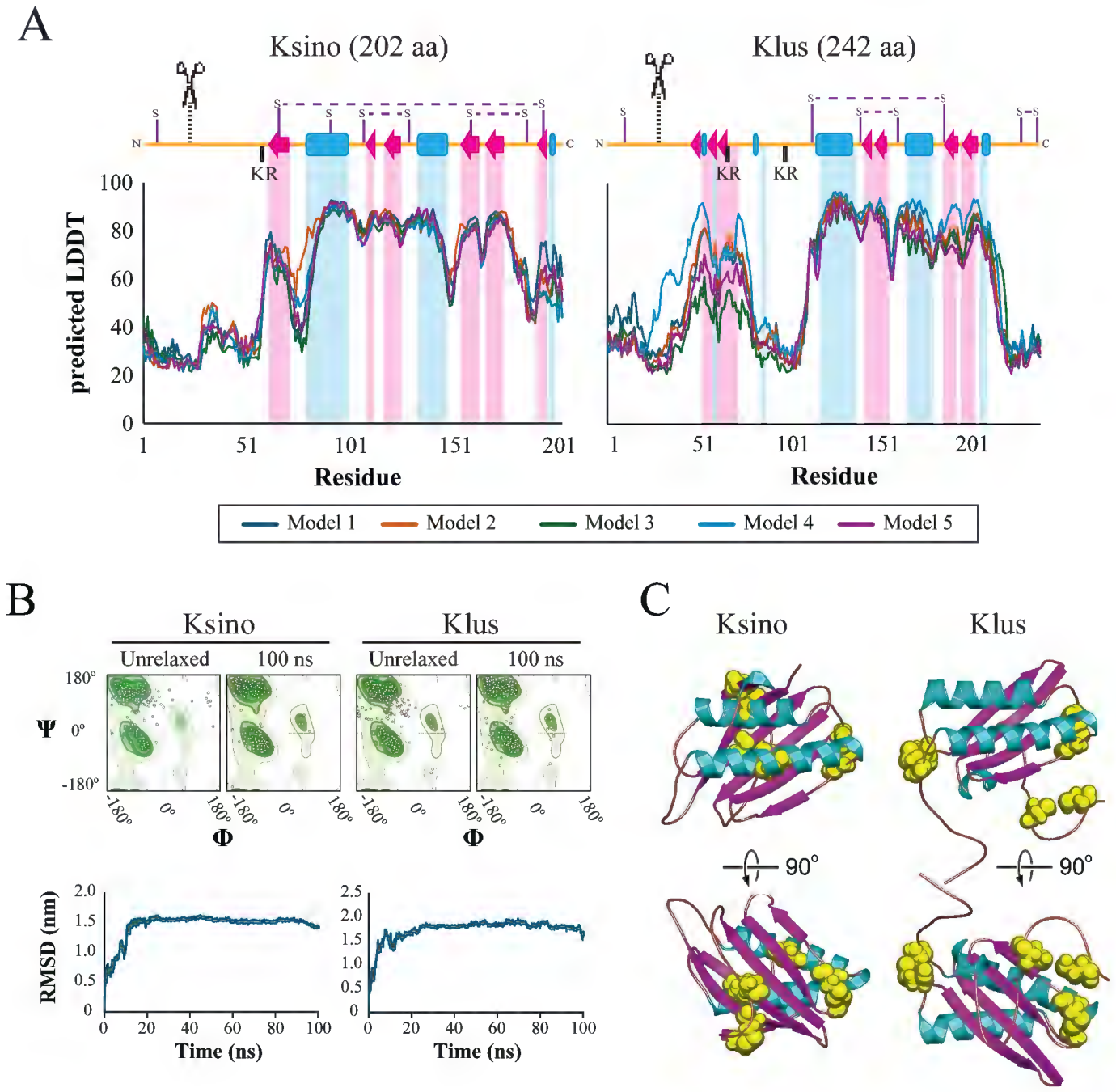
A
Ksino (202 aa)
Klus (242 aa)
N
C
KR
KR
KR
predicted LDDT
100
80
60
40
20
0
1
51
101
151
201
Residue
Model 1
Model 2
Model 3
Model 4
Model 5
B
Ksino
Klus
Unrelaxed
100 ns
Unrelaxed
100 ns
180°
Ψ
0°
-180°
-180°
0°
180°
Φ
RMSD (nm)
2.0
1.5
1.0
0.5
0
2.5
0
20
40
60
80
100
Time (ns)
C
Ksino
Klus
90°
90°

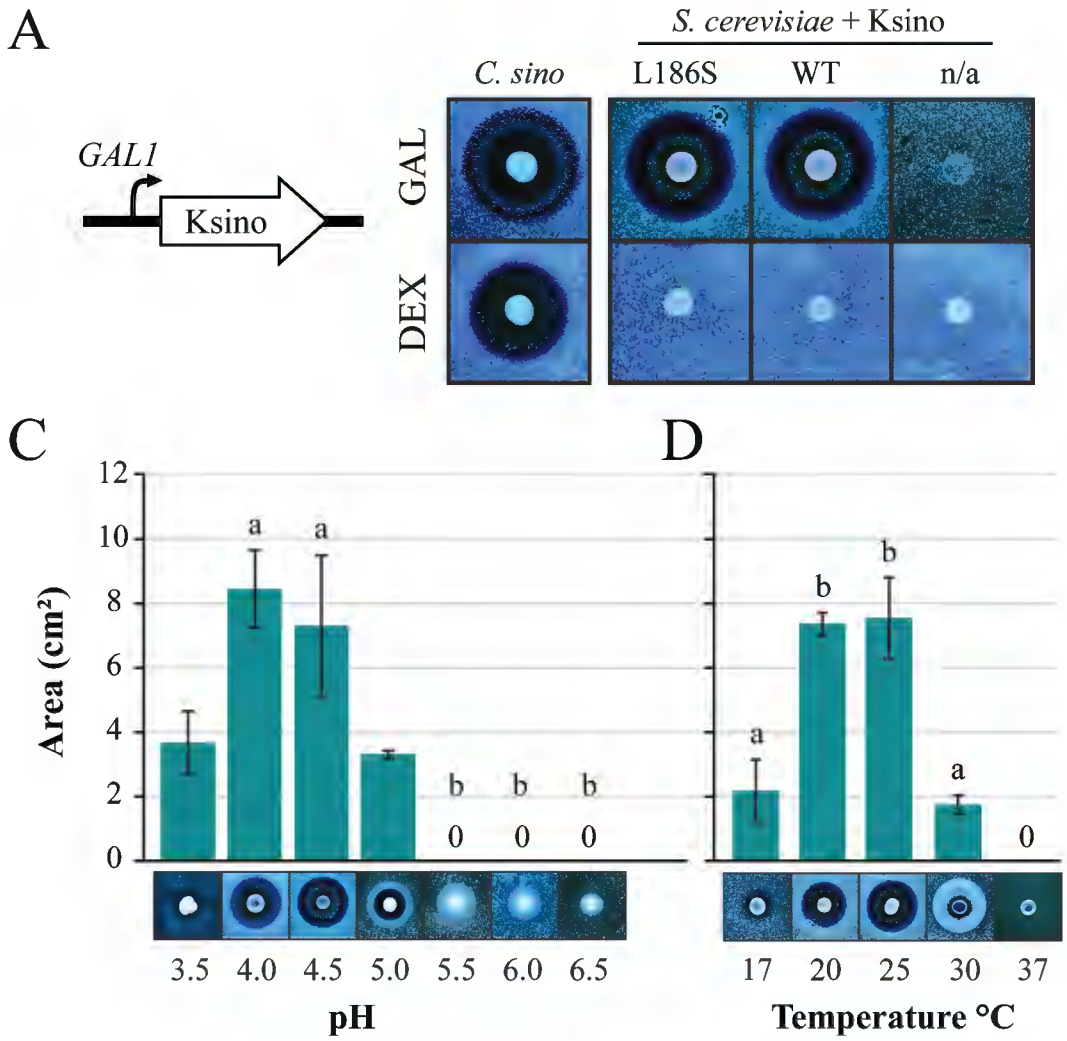
A
S. cerevisiae + Ksino
C. sino
L186S
WT
n/a
GAL1
Ksino
GAL
DEX
C
D
Area (cm²)
12
10
8
6
4
2
0
a
a
b
b
b
0
0
0
a
b
b
a
0
3.5
4.0
4.5
5.0
5.5
6.0
6.5
pH
17
20
25
30
37
Temperature °C